Marine and Petroleum Geology 92 (2018) 962–978

Contents lists available at ScienceDirect

Marine and Petroleum Geology

journal homepage: www.elsevier.com/locate/marpetgeo

Research paper

Geological and mechanical study of argillaceous North Sea chalk: Implications for the characterisation of fractured reservoirs

Ophélie Faÿ-Gomord[a], Michaël Verbiest[a], Eric Lasseur[b], Bruno Caline[c], Cécile Allanic[b], Fanny Descamps[d], Sara Vandycke[d], Rudy Swennen[a,*]

[a] Katholieke Universiteit Leuven, Earth and Environmental Sciences, Celestijnenlaan 200E, B-3001, Leuven-Heverlee, Belgium
[b] Bureau de Recherches Géologiques et Minières, Geology Department, Avenue Claude-Guillemin 3, F-45060, Orléans, France
[c] TOTAL France E. & P., Avenue Larribau, F-64018, Pau, France
[d] Université de Mons, Faculty of Engineering, Mining Engineering Department, Place du Parc 20, B-7000, Mons, Belgium

ARTICLE INFO

Keywords:
Chalk
Mechanical stratigraphy
Microtexture
Depositional facies
Petrophysics
Fractures

ABSTRACT

Argillaceous chalk intervals from the North Sea are characterised by matrix permeabilities lower than 0.2 mD and therefore they are defined as tight chalks. Hence, fracture networks within these chalks are of major importance to predict fluid flow and reservoir or seal behaviour. This study aims to understand the geological parameters controlling the chalk petrophysical and mechanical properties, using the outcrop analogue of the Cenomanian chalk at Cap-Blanc Nez (Northern France). Sedimentological, petrographic and petrophysical analyses were performed and show that the combination of the depositional environment and diagenetic imprint control the microtexture. Non carbonate content is ranging from 5 to 40% within the studied samples, and is critical for the diagenetic imprint. The fracture behaviour of the chalk was studied using a mechanical stratigraphy approach throughout the 70 m-thick succession, where a transition between lower Cenomanian argillaceous chalk and middle-upper Cenomanian pure chalk is exposed. Twenty-two mechanical units are distinguished and the amount of fractures crosscutting, initiating and terminating on mechanical interfaces quantified. Manual scanlines show that fracture spacing ranges from 17 to 232 cm. Mechanical interfaces are associated with lithological heterogeneities with strong microtextural contrasts, related to the non-carbonate content and/or degree of cementation. The mechanical units are thus defined either by deposition or diagenesis. The fracturing behaviour of about 10 m homogeneous pure chalk interval units, defined as DFZ (densely fractured zones) differs significantly from the rest of the succession. Large sigmoidal-shaped fractures are confined to those intervals, and a dense fracture network developed. Because of their plastic behaviour clay layers are able to accommodate part of the stress, whereas homogeneous pure chalk show a more brittle behaviour.

1. Introduction

Calcareous oozes have been deposited over large marine areas, from the Mesozoic till the present in sedimentary basins all over the world (Garrison, 1981). Chalk was deposited as such an ooze and is one of the most important carbonate rock types in NW Europe, playing a major economical role. Chalk is a major groundwater reservoir in NW Europe, yielding 8 million cubic metres daily (Downing et al., 2005) and a major hydrocarbon reservoir, especially in the North Sea. For example, estimates indicate that about 7 billion barrels of oil were originally in place in the Upper Cretaceous chalk of the Ekofisk Reservoir (North Sea) (Agarwal et al., 2000). Therefore, petrophysical properties and other rock characteristics of chalk reservoir intervals have been extensively studied and are fairly well known (e.g. Fabricius, 2007; Gommesen et al., 2007; Hardman, 1982; Scholle, 1977; Scholle et al., 1998; Vejbæk, 2002). Microporous chalk reservoirs are commonly characterised by high porosities (up to 50%) and low permeabilities (from 0.01 to 10 mD). However, only approximately 10% of the Upper Cretaceous/Lower Palaeocene Chalk Group in the central North Sea represents a conventional reservoir. The rest of the chalk was described as non-reservoir chalk (Damholt and Surlyk, 2004; Mallon and Swarbrick, 2002, 2008) or tight chalk (Faÿ-Gomord et al., 2016a; Lindgreen et al., 2012) which have permeability values lower than 0.2 mD (Bailey et al., 1999). Tight chalks have received relatively little attention since the discovery of chalk hydrocarbon reservoirs of the North Sea in the 1960s, despite forming the bulk of the chalk deposits. Recently there has been a growing interest in understanding the intrinsic properties of those low reservoir quality chalks that were

* Corresponding author.
E-mail address: rudy.swennen@kuleuven.be (R. Swennen).

https://doi.org/10.1016/j.marpetgeo.2018.03.037
Received 3 November 2016; Received in revised form 11 March 2018; Accepted 28 March 2018
Available online 03 April 2018
0264-8172/

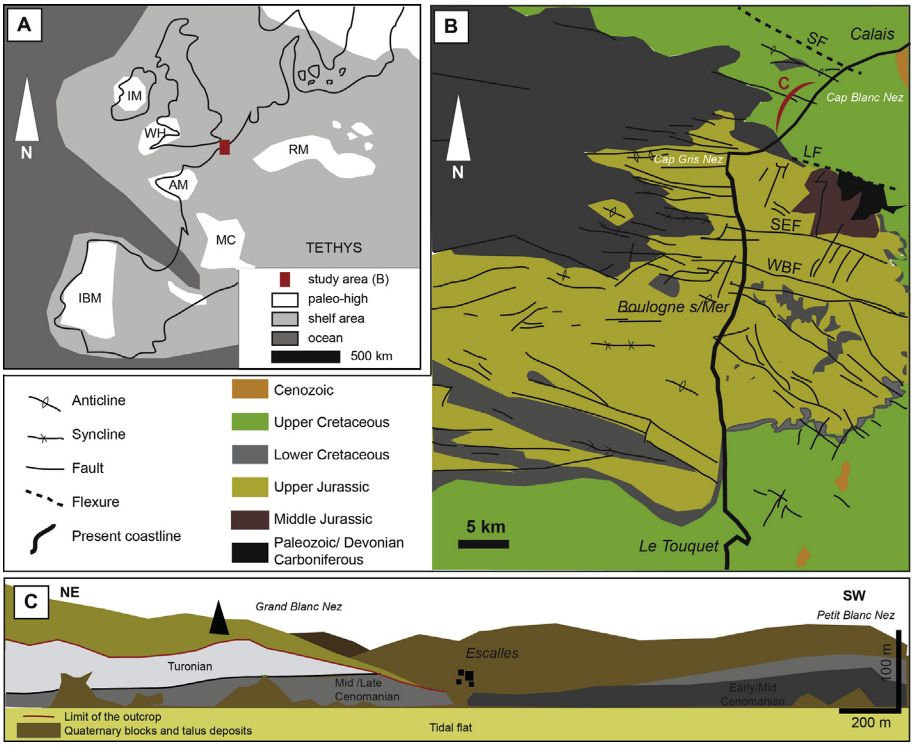

Fig. 1. (A) Palaeogeography map of western Europe during the middle Cenomanian (after Wendler et al., 2002); AM = Armorican Massive, WH = Wales High, IBM = Iberian Massive, IM = Irish Massive, MC = Massive Centrale, RM = Rheinish Massive. (B) Geological map of northern France, showing the extent of the Weald–Boulonnais Basin. (after Mansy et al., 2003) (C) Schematic profile of the cliffs along section C (after Amédro and Robaszynski, 2001).

previously identified as potential intrareservoir seals (Damholt and Surlyk, 2004; Fabricius, 2001; Gennaro et al., 2013; Hjuler and Fabricius, 2009; Jakobsen et al., 2004; Madsen, 2010; Røgen and Fabricius, 2002).

In such low permeability rocks, fractures are the primary pathway for fluid flow (Nelson, 1985), and the role of structural features as preferential flow pathways in chalk have been proven to be important in reservoir studies (e.g. Bear, 1993; Travis, 1984). In layered rocks it has been shown that the opening and the intensity of joint fracturing is controlled by stratigraphy. This was highlighted by Underwood et al. (2003) and Rustichelli et al. (2012), who defined a mechanical unit as a unit representing one or more sedimentary beds that fracture independently from other units. These mechanical units are bounded by mechanical interfaces, which are commonly related to sedimentary contrasts, although sedimentary boundaries do not always define mechanical interfaces. An example where the concept of mechanical stratigraphy has been applied to chalk are the deeply buried Austin chalks in Texas, where mechanical interfaces correspond to thick marl interlayers (Cooke et al., 2006).

In the subsurface, tight chalk intervals constrain fluid flow, acting as seals or as unconventional reservoirs depending on their fracture patterns. In order to accurately characterise their heterogeneity and to determine fundamental controls on fracturing behaviour of argillaceous chalks, outcrop analogue studies are essential. Thus, a multidisciplinary approach was used on the Cenomanian argillaceous chalk cliffs of Cap Blanc-Nez in Northern France. Deposits are characterised by a high non-carbonate content (up to 38%) resulting in very low permeabilities (as low as 0.04 mD) (Faÿ-Gomord et al., 2016a). Previous studies of this outcrop provide a detailed stratigraphical framework (Amédro and Robaszynski, 2001; Robaszynski and Amédro, 1986) and a detailed understanding of the clay fraction (Deconinck et al., 1989, 2005; Deconinck and Chamley, 1995). However, data on the petrographic, petrophysical and microtextural properties of the Cap Blanc-Nez chalk are limited to Doremus (1978), who described chalk microtextures based on SEM observations. This author highlighted the influence of porosity and clay content on mechanical properties, as well as the importance of grain contacts on the intrinsic cohesion of the rock. However, the relationship between the geological context, e.g. depositional and diagenetic history of the samples and their microtextural properties was not emphasized.

This study aims to better understand the geological history of Cap Blanc-Nez chalk, from depositional setting, through diagenesis and fracturing. Chalk porosity and permeability properties are assessed using sedimentological and petrographic analyses. In order to characterise the fracture network and define the mechanical interfaces, a mechanical stratigraphy study was performed. The latter provides essential information regarding fluid flow, since a proper characterisation of the dual permeability of pores and fractures is essential in order to accurately model fluid flow in aquifers, hydrocarbon reservoirs or apparent aquacludes and seals. The Cap Blanc-Nez outcrop allows an understanding of the behaviour of argillaceous chalk intervals in NW Europe and especially their equivalents in hydrocarbon fields of the North Sea. This study reveals the prominent impact of the variations in non-carbonate phases on the characteristic behaviour of a layered chalk succession, influencing both petrophysical and rock mechanical properties.

2. Geological settings

The field study focused on the 5 km long chalk cliffs of Cap Blanc-Nez (northern France), which is located in the Boulonnais area, in the NW part of the Paris Basin. The Paris Basin was part of the NW European Chalk Sea, which formed a large basin in western Europe known as the Anglo-Paris Basin. This intracratonic basin was mainly characterised by thermal subsidence, following Permian–Triassic tectonic extension (Brunet and Le Pichon, 1982; Le Solleuz et al., 2004). The basin is currently bounded by the Brabant Massif to the northeast which became flooded during the Late Cretaceous, the Central Massif to the south, and the Armorican Massif to the west (Fig. 1).

2.1. Sedimentological setting

The 70 m thick succession of Cap Blanc-Nez is the reference section for the Cenomanian in this part of the Anglo-Paris Basin (Robaszynski

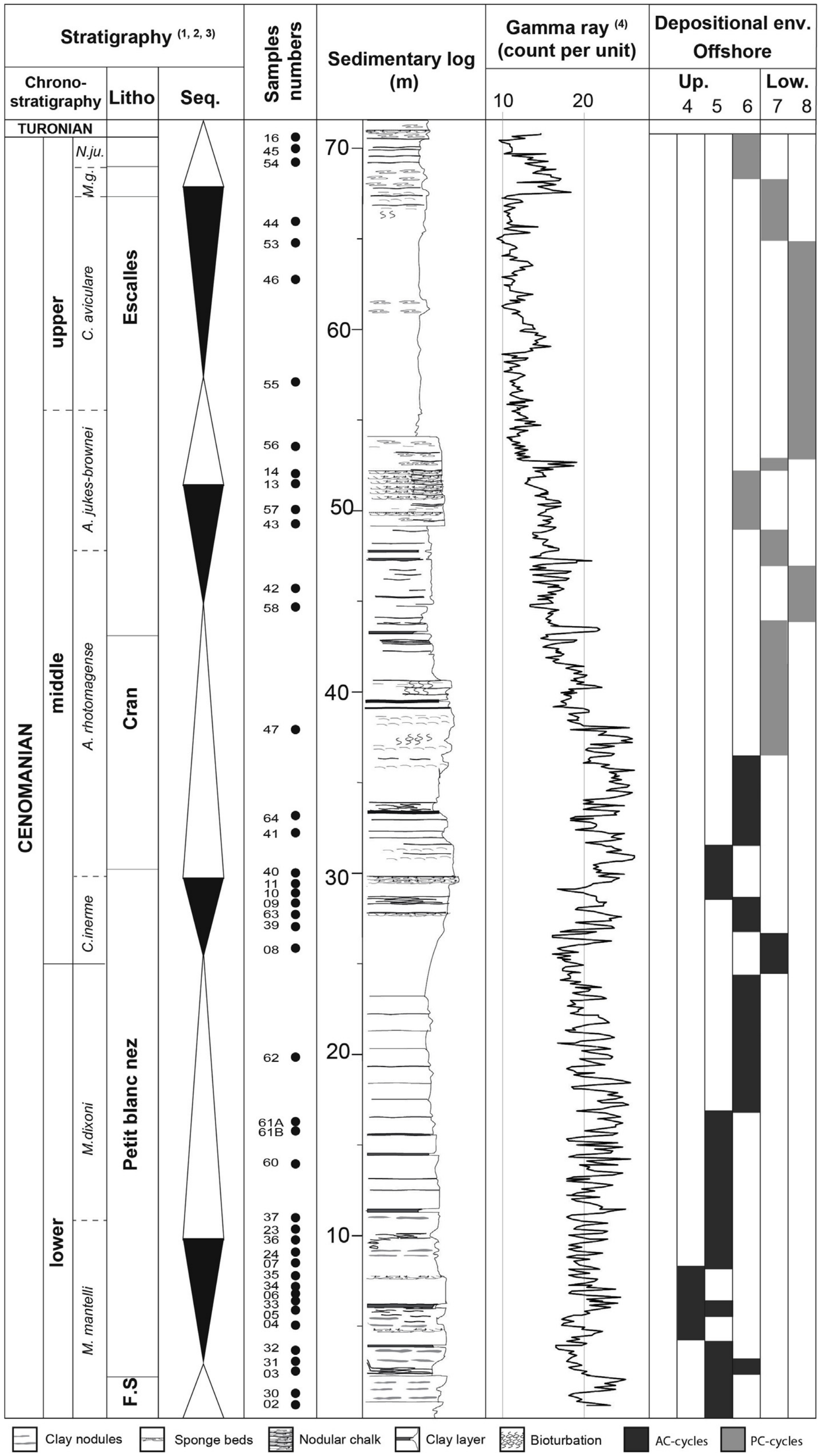

Fig. 2. Sedimentological log of the Cap Blanc-Nez Cenomanian chalks. Stratigraphy from Robaszynski and Amédro (1986, 1993) and Amédro and Robaszynski (2001) [1,2,3]. Biostratigraphy based on ammonites. Gamma-ray measurements from Gräfe (1999) [4]. Location of the depositional environment along a carbonate ramp are from the more proximal facies (4) to the more distal (8). Sequence stratigraphy based on depositional facies. Abbreviation: F.S. = Formation Strouanne, *M.g.* = *Metoicoceras geslinianum*, *N.j.* = *Neocardioceras judii*.

Table 1
Abbreviations used throughout the manuscript by order of appearance.

DF	Depositional Facies
MT	Microtexture
IR	Insoluble Residue
DFZ	Densely Fractured Zone
SEM	Secondary Electron Microscope
UCS	Uniaxial Compressive Strength
HCS	Hummocky Crossed Stratification
AC-cycle	Argillaceous Chalk sedimentary cycle
PC-cycle	Pure chalk sedimentary cycle
MFS	Maximum Flooding Surface
MI	Mechanical Interface
MU	Mechanical Unit

and Amédro, 1986). Deposition originally took place in an outer shelf setting characterised by continuous sedimentation of metre-thick chalk/marl alternations. During the Cenomanian, a continuously rising sea level led to the worldwide expansion of shelf seas (Haq et al., 1987). This event was expressed locally as chalk deposition on a progressively developing carbonate ramp, with deposition of chalk and a significant siliciclastic input from the Armorican Massif to the south (Juignet, 1974) and the Brabant Massif to the northeast (Deconinck and Chamley, 1995). Lower Cenomanian chalks have a relatively high siliciclastic content because they were deposited adjacent to deltaic and estuarine sediments, located in the Biscay Bay during the Late Cretaceous (Guillocheau et al., 2000). Cap Blanc-Nez chalk deposits range from glauconitic argillaceous bioclastic chalks in the lower Cenomanian to pure white chalks that were deposited during the late Cenomanian (Amédro and Robaszynski, 1993). The Cenomanian chalks in the study area have been subdivided into five regional formations (Fig. 2), namely: (I) Strouanne Formation, 2 m thick at the base of the lower Cenomanian, also called glauconitic chalk; (II) Petit Blanc-Nez Formation of early Cenomanian age and base of the middle Cenomanian, composed of about 30 m of chalk/marl alternations; (III) Cran Formation, part of middle Cenomanian consisting of about 10 m of chalk/marl cycles with high carbonate content; (IV) Escalles Formation, part of middle Cenomanian and upper Cenomanian made of 30 m of thin rhythmically bedded chalk; (V) Crupes Formation, 1–2 m thick corresponding to the uppermost Cenomanian, overlain by the Turonian Plenus Marls.

A cyclostratigraphic study performed on middle and upper Cenomanian chalks relates the variations in the planktonic foraminifera to plankton productivity, associated with water depth (Gräfe, 1999). The clay-mineralogy of the Cenomanian chalks of the Boulonnais was studied by Deconinck et al. (1989) and Deconinck and Chamley (1995). Detrital clays found in the chalk include illite, smectite and kaolinite (Deconinck and Chamley, 1995). Smectite dominance in the lower Cenomanian succession changes to illite and kaolinite dominance upwards into the middle Cenomanian succession (Deconinck et al., 1989). Metre-thick cycles are recorded in gamma-ray logs acquired by Gräfe (1999) on the whole Cenomanian chalk section of Cap Blanc-Nez (Fig. 2).

2.2. Structural context and fracture network

Several patterns of master joints and normal faults with NW–SE orientation are observed in the Cenomanian–Santonian chalks in the Boulonnais (Vandycke and Bergerat, 1992) and relate to the NE–SW Oligocene extension phase, clearly identified in the whole NW European platform in terms of faulting and master jointing (Bevan and Hancock, 1986) or in geomorphological studies. The NE–SW extension was active since the end of the Cretaceous until the Neogene.

A palaeostress study based on fault-slip analyses recorded in the Cretaceous formations of the Boulonnais revealed an extensive regime interrupted time-to-time by inversion tectonics along the Nord-Artois-Shear Zone (Bergerat and Vandycke, 1994; Colbeaux, 1974; Vandycke and Bergerat, 1992; Vandycke, 2002). The palaeostress evolution in the Boulonnais area showed that several tectonic events took place during the Cretaceous. The inversion of this area took place during the Cenozoic. A late Eocene inversion has been documented, although it could be multiphase starting in the early Palaeocene (Mansy et al., 2003; Briais et al., 2016).

3. Methodology

3.1. Sedimentology

Sedimentological logging was performed on the 70 m thick section of the Cenomanian chalks. Facies interpretation was performed following Lasseur et al. (2009). Metre-scale cycles were identified and classified based on depositional facies and hiatal surfaces. Depositional facies (DF) classification is based essentially on shell concentration, sedimentary structures, texture and faunal content (faunas, ichnology) observed both in the field and in thin-section. Hiatal surfaces are classified according to their type (hardgrounds, firmgrounds and softgrounds), ichnofacies and the occurrence/absence of an erosion surface on top of these condensed levels. For coherence purposes, the depositional facies (DF) designations used by Lasseur et al. (2009) were maintained and range from the shallowest/coarsest DF1 to the deepest/finest DF7. However, the reader should be aware that Lasseur et al. (2009) developed this classification for sedimentary cycles based on Normandy outcrops where due to the palaeogeographic setting terrigenous input is significantly lower than in present study area. In order to integrate the distinct argillaceous and pure chalk facies characteristic of Cap Blanc-Nez, sedimentary cycles were defined as PC-cycles for pure chalk and AC-cycles for argillaceous chalk (Table 2). Other abbreviations used throughout this paper are summarised Table 1.

In the field, 42 samples were collected and 30 μm thin-sections were prepared. Samples were impregnated under vacuum with a fluorescent epoxy resin to highlight the porous network, when studied by fluorescent incident light microscopy. Lasseur et al. (2009) positioned their cycles on a water depth profile, based on both hydrodynamic characteristics, provided by shell concentration or sedimentary structures, and echinoid palaeoecology. The vertical succession of facies/cycles was thus used to build a 1D sequence stratigraphic framework according to the methodology of high-resolution sequence stratigraphy (Homewood et al., 1992).

3.2. Petrography and insoluble residue measurements

Samples were impregnated under vacuum with a fluorescent epoxy resin to highlight the porous network, when studied by fluorescent incident light microscopy. Additionally, an EM XL30 FEG field emission Scanning Electron Microscope (SEM) was used to observe the fresh surfaces of the samples to identify microporosity and to study microtextural features, especially non-carbonate content and cements. Throughout this paper, the term *microtexture* describes the texture of the chalk matrix, as observed under SEM, while *texture* refers to the Dunham sedimentary texture classification. Acid-insoluble residues of the samples were obtained by dissolving roughly crushed samples of chalk in 2 M hydrochloric acid followed by washing of the residue with deionised water (Hjuler and Fabricius, 2009). Forty-two samples of Cap Blanc-Nez Cenomanian chalk were characterised both in terms of depositional facies based on thin-section petrography and microtexture analyses based on SEM observations.

3.3. Petrophysics and geomechanics

Helium porosity and Klinkenberg's corrected permeability measurements were performed on 38 and 36 samples, respectively, and uniaxial compressive strength (UCS) measurements were performed on

Table 2
Characteristics of each depositional facies (after Lasseur et al., 2009).

Depositional Facies	Macroscopic observation			Microscopic observation						Samples names	Sedimentary cycles		
	Faunas		Sedimentary structures	Dunham texture	Macrofaunas		Microfaunas	Other elements	Sedimentary structures		Hital surfaces associated	Possible cycles	Lasseur et al. (2009)
	Nature	Preservation			Nature	Preservation							
DF2/3	Bryozoans, Echinids and Bivalves	Disarticulated and broken	Planar to HCS laminations	Fine to medium sand packstone	Abundance of Echinoderms, some Inoceramids, Bryozoans and unidentified Bivalves	Highly corroded and intensely broken Echinoderms, preserved Bryozoan and brachiopods	Rare calcispheres and foraminifera	Iron oxyde, detrial glauconite, quartz sands	Not observed in thin-section	CB30, CB03, CB04, CB06, CB34, CB36, CB11	FG1/SG1	AC-4	C4
DF3	Echinids, Brachiopods, Bivalves, Bryozoans	Intensely broken	Planar to slightly undulating HCS laminations	Fine sand packestone -wackestone	Abundance of Echinoderms, some Inoceramids, Bryozoans and unidentified Bivalves	Highly corroded and intensely broken Echinoderms, preserved Bryozoan and brachiopods	Calcispheres and foraminifera	Rare quartz, iron oxyde and glauconitic grains	Rare planar alignements of the bioclasts	CB02, CB31, CB32, CB33, CB35, CB37, CB60, CB61B	FG1/SG1	AC-4	C4
DF4	Bivalves, Brachiopods, Echinids, some Bryozoans	Intensely broken, sometimes less fragmented	Rare laminations, burrowed	Silt to fine sand wackstone -packstone	Echinids, Brachiopods, Bivalves and sponge spicules	Highly corroded and intensely broken Echinoderms, well preserved Bryozoan and Brachiopods	Calcispheres and foraminifera	Rare quartz and glauconitic grains	Some planar alignements of the bioclasts	CB23, CB61A, CB62, CB07, CB039, CB63, CB09, CB40, CB41, CB64	FG2/SG2 FG1	AC-5 AC-6	C5 C6
DF5	Few bivalves, Echinids, Brachiopods, some Bryozoans	Mainly broken, some well preserved shells	Structureless, highly burrowed	Silt wackestone	Echinids, Inoceramids and sponge spicules	Highly corroded and intensely broken Echinoderms, moderately to highly corroded other bioclasts	Calcispheres and sponge spicules -dominated, with some foraminifera	None	Some preferential orientation and alignements of bioclasts (especially sponge spicules and calcispheres)	CB24, CB10, CB44, CB54, CB45, CB16	SG2 FG2	AC-7 PC-6	C7 TC6
DF6	Few bivalves, Echinids, Brachiopods, some Bryozoans	Well preserved shell, occasionally broken	Structureless, highly burrowed	Mudstone-Wackestone	Echinids, Inoceramids, sponge spicules and Mollusk fragments	Corroded and broken bioclasts	Abondance of calcispheres, sponge spicules, and some foraminifera	None	None	CB47, CB43, CB57, CB13, CB14	SG2	PC-7	TC7
DF7	Almost no macrofauna	NA	None	Mudstone	Very rare Innoceramids and Echinids fragments.	Corroded and intensely broken bioclasts. Sometimes hardly recognizable.	Some rare calcispheres and foraminifera	None	None	CB08, CB42, CB56, CB55, CB46, CB53	None	PC-8	TC8

29 samples. For a detailed methodology readers are referred to Faÿ-Gomord et al. (2016b).

3.4. Mechanical stratigraphy

In order to characterise the fracture properties of the chalk succession, manual scanlines were performed. These scanlines were acquired in the field for every accessible mechanical unit. Mechanical units were defined between two mechanical interfaces for which less than 3/5 of the fractures were crosscutting. The outcrop is orientated NE–SW, and the open-mode fractures measured within the scanlines belong to the NW–SE family defined by Vandycke (2002), which is perpendicular to the cliff outcrop and the scanlines. Therefore, no Terzaghi correction was applied to the collected dataset. The very small dip of the chalk deposits, of about 3°, makes it possible to access the whole section of Cenomanian chalk and to perform scanlines along an outcrop more than 5 km in total length. Length of the scanlines was based on Representative Elementary Length (REL) curves acquired in the field together with fracture spacing measurements. Previous studies have shown that fracture density depends on distance to faults (Vermilye and Scholz, 1998) and tends to increase towards the fault core within the fault-damage zone (Caine et al., 1996). The thickness of the latter depends on several parameters including the fault displacement or throw (Faulkner et al., 2010). Therefore, scanline measurements were performed away from fault zones, although major damage zones of major faults are very limited in Cap Blanc-Nez. For each scanline, the thickness of the mechanical unit was measured and the fracture counting was performed in the middle of each unit. In order to assess the liability of the scanline measurements, any clustering effect had to be excluded. Therefore, the coefficient of variation (C_V) of each scanline was calculated, following Gillespie et al. (1999, 2001). Cv is defined as the ratio of the standard deviation to the mean fracture spacing. Clustering is considered to be present if $Cv > 1$, meaning that the standard deviation would be higher than the average fractures spacing. Fracture spacing was measured along the 22 mechanical units and the percentage of fractures crosscutting, initiating and terminating at each mechanical interface was quantified.

4. Results

4.1. Sedimentology

4.1.1. Depositional facies

Six depositional facies were distinguished (Table 2). DF1 identified by Lasseur et al. (2009) is not present in Cap Blanc-Nez. DF2–3 (packstone with many bioclasts) to DF4 (fine wackestone-packstone with small bioclasts and calcispheres) are identified within the argillaceous chalk succession, while DF4 to DF6 (mudstone-wackestone dominated by calcispheres and sponge spicules) are present in both argillaceous and pure chalk and DF7 (mudstone) corresponds to pure chalk. As in the Normandy outcrops, from DF2–3 to DF5, abundance of broken shells and the coarser grain size as well as better sorting reflect a higher hydrodynamic setting. As described in detail by Lasseur et al. (2009), sedimentary features such as planar or hummocky cross-stratified (HCS) laminations are present in argillaceous chalk in DF2–3 (Fig. 3). Winnowing of smaller-particles resulted in bioclast concentration, such as in DF5 which is dominated by calcispheres. Facies DF2/3 to DF4 were interpreted by Lasseur et al. (2009) as upper offshore deposits. Glauconite grains are observed in thin-sections within DF2-3 (very abundant), DF3 (common) and DF4 (sparse). Iron oxides, which are likely of secondary origin, are found associated with centimetre-size marcassite nodules (DF2–4) and/or with rare framboidal pyrite in thin-section. In contrast, DF6 and DF7 facies do not display evidence of sorting, as demonstrated by their mudstone texture. Macrofossils are rare to absent and the facies are dominated by open-sea microfossils, revealing a deeper depositional setting. DF7 consists of pure mudstones composed of coccolith fragments deposited by settling. DF6 and DF7 are thus associated with lower offshore environments. Characteristic microfacies of each depositional facies are illustrated in Fig. 4.

4.1.2. Hiatal surfaces

In Cap Blanc-Nez, hiatal surfaces essentially consist of more or less pronounced firm- and softgrounds. Firmgrounds are typically associated with more proximal facies. They mainly occur in the lower part of the section and are typically associated with sponge beds and erosion on top (FG1 type of Lasseur et al., 2009). They are more scattered in the upper part of the succession, where hiatal surfaces are less pronounced and expressed by softgrounds. Two prominent firmgrounds are present in the middle Cenomanian and display both deformed *Thalassinoides* burrows and poorly deformed vertical burrows. Around the middle/upper Cenomanian boundary, a condensed interval, several metres thick, corresponds to several stacked firmgrounds. The softgrounds correspond to distinct surfaces overlying *Thalassinoides*-bioturbated chalks which are characterised by poorly defined, highly deformed burrows. Softgrounds are poorly expressed surfaces associated with fine grained mudstone.

4.1.3. Sedimentary cycles

Depositional facies and hiatal surfaces are organized according to recurrent cyclic patterns, which form sedimentary cycles (Lasseur et al., 2009). The relationship between hiatal surfaces, depositional facies and sedimentary cycles are shown in Table 2, along with the correspondence between the terminology used in this study and the one used by Lasseur et al. (2009) in the original classification. Sedimentary cycles range from the shallowest (AC-4) to the deepest (PC-8), along a storm-dominated carbonate ramp (Fig. 5). Some cycles formed below storm waves base (AC-4 to AC-6 and PC-6), whereas others developed above it (PC-7 and PC-8). Hiatal surfaces are more developed in the more proximal cycles. The occurrence of the different sedimentary cycles in the Cenomanian chalk succession are represented in Fig. 2. AC-cycles are related to a proximal depositional environment based on their faunal content and sedimentary features (Fig. 3). These several decimetres thick cycles, commonly grouped in series of 4–5 cycles, are usually topped by sponge beds highlighting a hiatal surface (Fig. 3B). They are also associated with an increase in clay content as reflected in the gamma-ray log (Gräfe, 1999, Fig. 2). In pure chalk, the sedimentary cyclicity is highlighted in the field by the regular occurrences of marl-seams (Fig. 3- E) which preferentially develop on top of bioturbated intervals. The *C. naviculare* zone (Fig. 2), at the base of the upper Cenomanian, is characterised by sedimentary cycles PC-8 (DF7: mudstone, no hiatal surfaces) and reflects the maximum transgression of the Cenomanian (Juignet, 1974).

4.1.4. A transgressive trend with higher order sequences

Overall, the evolution of both macro- and microfacies through the 70 m-thick Cenomanian succession displays a transgressive trend, with several higher order sequences. The maximum flooding surfaces are associated with the deepest facies of the section. They are recorded at 25 m (transition lower/middle Cenomanian), 45 m (middle Cenomanian) and 57 m (upper Cenomanian). The sequence stratigraphy obtained from sedimentary cycle associations and their related water-depth model fits with the sequences proposed for the same outcrop by Robaszynski et al. (1998). Their interpretation in terms of sequence stratigraphy is essentially based on non-carbonate content and biostratigraphy, highlighting the strong correlation between the insoluble residue content and the transgression that precluded siliciclastic input to the basin.

4.2. Insoluble residue and microtextures

Insoluble residue (IR) contents range from 5 to 38% within the

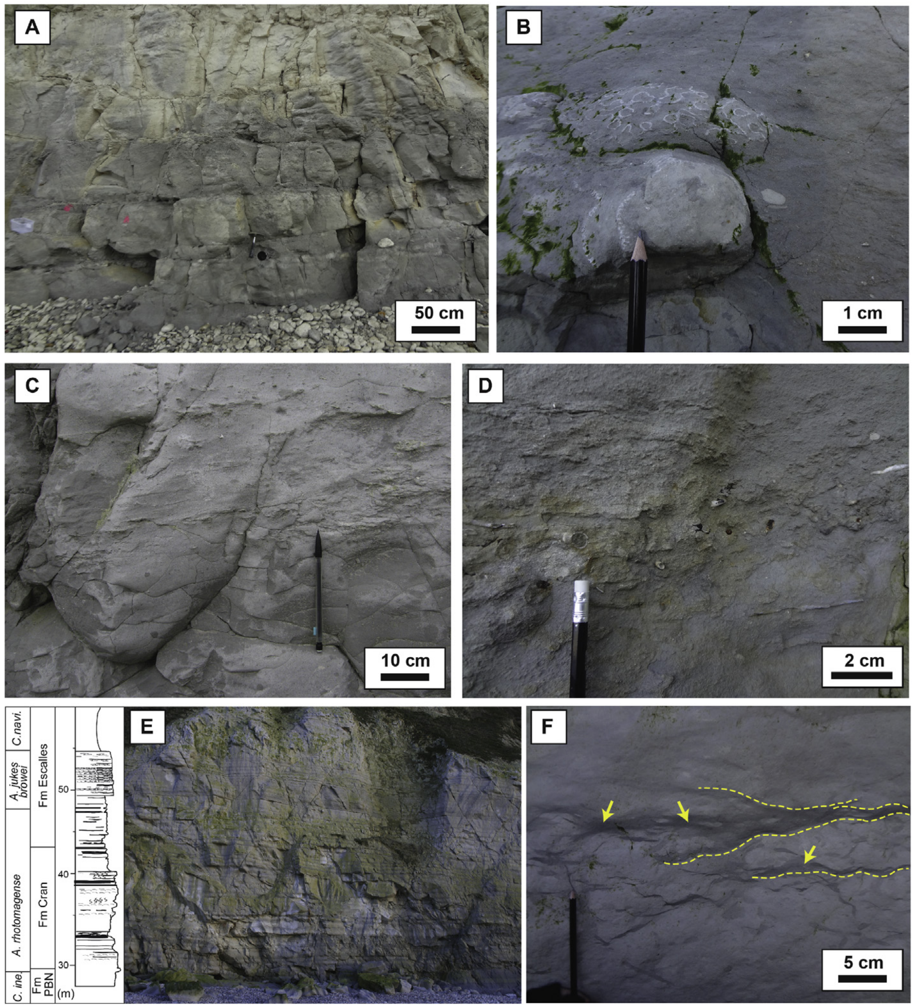

Fig. 3. (A) Basal Cenomanian sedimentary facies (DF2-3 to 3, cycle AC-4 and AC-5) (B) Sponge bed from a firmground, characteristic of AC-4/AC-5 sedimentary cycles (C) HCS laminations characteristic of DF 2–3 (D) Storm deposits with many bioclasts (E) Overview of middle/upper Cenomanian deposits. The cyclicity is highlighted by darker marl-seams horizons (F) PC-7 sedimentary cycles with marl-seams features (yellow arrow). (For interpretation of the references to colour in this figure legend, the reader is referred to the Web version of this article.)

studied chalks. From the lower Cenomanian until the *A. rhotomagense* zone (middle Cenomanian), the IR values range between 10 and 38%. Lower non-carbonate contents are associated with hiatal surfaces, such as firmground samples CB10 and CB39 (Appendix 1) that contain 10% and 11% IR, respectively. Starting from the *A. rhotomagense* zone until the top of the upper Cenomanian, IR content ranges from 5 to 15%, with values from 10 to 15% for chalk with marl-seams and from 5 to 8% for interlayered clean chalk (Appendix 1).

Microtexture classes were previously defined by Faÿ-Gomord et al. (2016b), based on SEM observations of the degree of cementation and non-carbonate content measurements. Five microtextures (MT) are recognized within the Cenomanian chalks of Cap Blanc-Nez (Fig. 6):

- MT1: poorly to uncemented pure chalk. The non-carbonate content is low (below 8%), as well as the degree of cementation. Cement overgrowths on coccolith particles are uncommon, and authigenic calcite crystals are rare to absent. Contacts between grains are essentially punctic and coccoliths are well preserved. Intraparticular porosity of foraminifera and calcispheres is preserved.
- MT2: moderately cemented pure chalk. Samples are characterised by low non-carbonate content (below 8%) and a higher degree of cementation. Cement overgrowth is common, as well as authigenic calcite crystals. Contacts between grains are serrated, and the chambers of foraminifera and calcispheres are cemented.
- MT3: moderately cemented argillaceous chalk. Samples are characterised by a very high non-carbonate content (> 20%), dominated by clays. Clays are mostly observed as thin undulated flakes of 1–5 µm in size, non-orientated and dispersed in the matrix, sometimes larger clay sheets partly coat some carbonate grains.
- MT4: poorly cemented argillaceous chalk. The microtexture is very similar to MT3. However, SEM observations of MT4 samples reveal the presence of clay flakes orientated parallel to the bedding.
- MT5: highly cemented argillaceous chalk. MT5 samples display high non-carbonate content (from 8 to 20%) and a high degree of cementation. Authigenic calcite crystals are present in the matrix. Contact between grains ranges from punctic to fused. Microns-thick cemented zones are regularly observed in the samples. Coccoliths are rare, but usually well preserved, with common cement overgrowths. Clay particles are present as flakes, as in MT3 and 4, but do not display any recognizable orientation.

As previously established, microtextures are controlled by both depositional settings and diagenetic alteration (e.g. Fabricius et al., 2007; Faÿ-Gomord et al., 2016a, b). Fig. 7 illustrates the relationship between depositional facies and microtextures. Although there is no clear correlation between one depositional facies and one single type of microtexture, it appears that DF2–3, DF3 and DF4 preferentially show clay-rich microtextures MT3, MT4 and MT5. DF5, DF6 and DF7 are

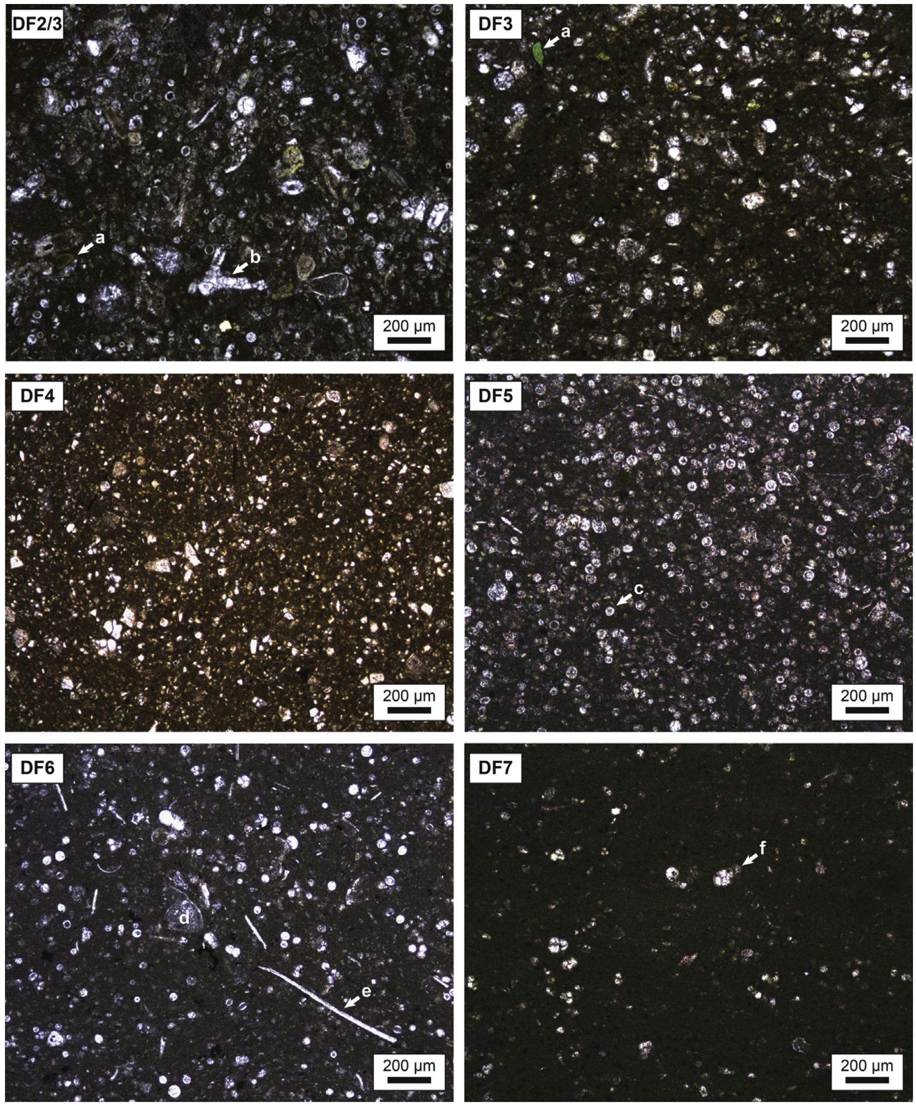

Fig. 4. Microphotograph of typical depositional facies (DF2-3) Packstone with many bioclasts, glauconitic grains and some quartz (DF3) Wackestone-packstone with bioclasts, calcispheres and glauconitic grains (DF4) Fine wackestone-packstone with small bioclasts, calcispheres; displaying some bioclasts alignments (DF5) Wackestone dominated by calcispheres (DF6) Mudstone-wackestone dominated by calcispheres and sponge spicules (DF7) Mudstone with rare calcispheres and foraminifera.

dominated by pure microtextures MT1 and MT2. In terms of stratigraphic distribution, MT3–5 are dominant in the lower to middle Cenomanian (*A. rhotomagense* zone) strata, when the clay input from the land was significant. MT1 and MT2 are prevalent from the middle Cenomanian and upward, and were deposited during a period of low detrital input. In the upper portion of the strata, clay-rich microtextures are related to pressure-dissolution horizons. They are representative of centimetre-thick intervals where marl-seams developed marked by concentrated insoluble residue.

4.3. Petrophysics and geomechanics

Porosity values of the samples range from 17 to 37%. Permeability values range from 0.04 to 2.3 mD with more than 70% of the samples qualifying as tight chalks, according to the Joint Chalk Research definition, thus holding permeability values lower than 0.2 mD (Bailey et al., 1999).

Depositional facies impacts porosity and permeability (Fig. 8). Samples from DF5 (calcisphere-rich wackestone) cluster together, as well as DF6 (calcisphere-rich mud-wackestone) (Fig. 8). The impact of depositional setting on petrophysical properties has been proven in chalks, especially the contrast between autochthonous and allochthonous deposits (Kennedy, 1987; Taylor and Lapre, 1987). The latter commonly exhibit better reservoir properties. The petrographic and petrophysical observations on the Cap Blanc-Nez chalks show that small depositional facies variations influence petrophysical properties. The changes in grain size and sorting, controlled by deposition, especially control the petrophysical properties. Microtexture also impacts porosity and permeability (Fig. 8), however, of each of those depositional facies types, which are classified according to hydrodynamics, the samples exhibiting argillaceous microtexture display lower porosity and permeability values within all depositional facies. Several studies demonstrate that microtexture, especially the degree of cementation and clay content, controls petrophysical properties (e.g. Fabricius, 2007; Faÿ-Gomord et al., 2016a, b; Mortimore and Fielding, 1990). The degree of cementation and clay content are inversely related to porosity and permeability values, MT1 samples display the highest values with porosities ranging from 33 to 37% and permeabilities ranging from 0.3 to 2.3 mD. MT2 cementation reduces porosity (17–27%) and permeability (0.15–0.4 mD). MT5 samples, which are characterised by both a high degree of cementation and high non-carbonate content, display tight chalk permeability values ranging from 0.04 to 0.13 mD, and

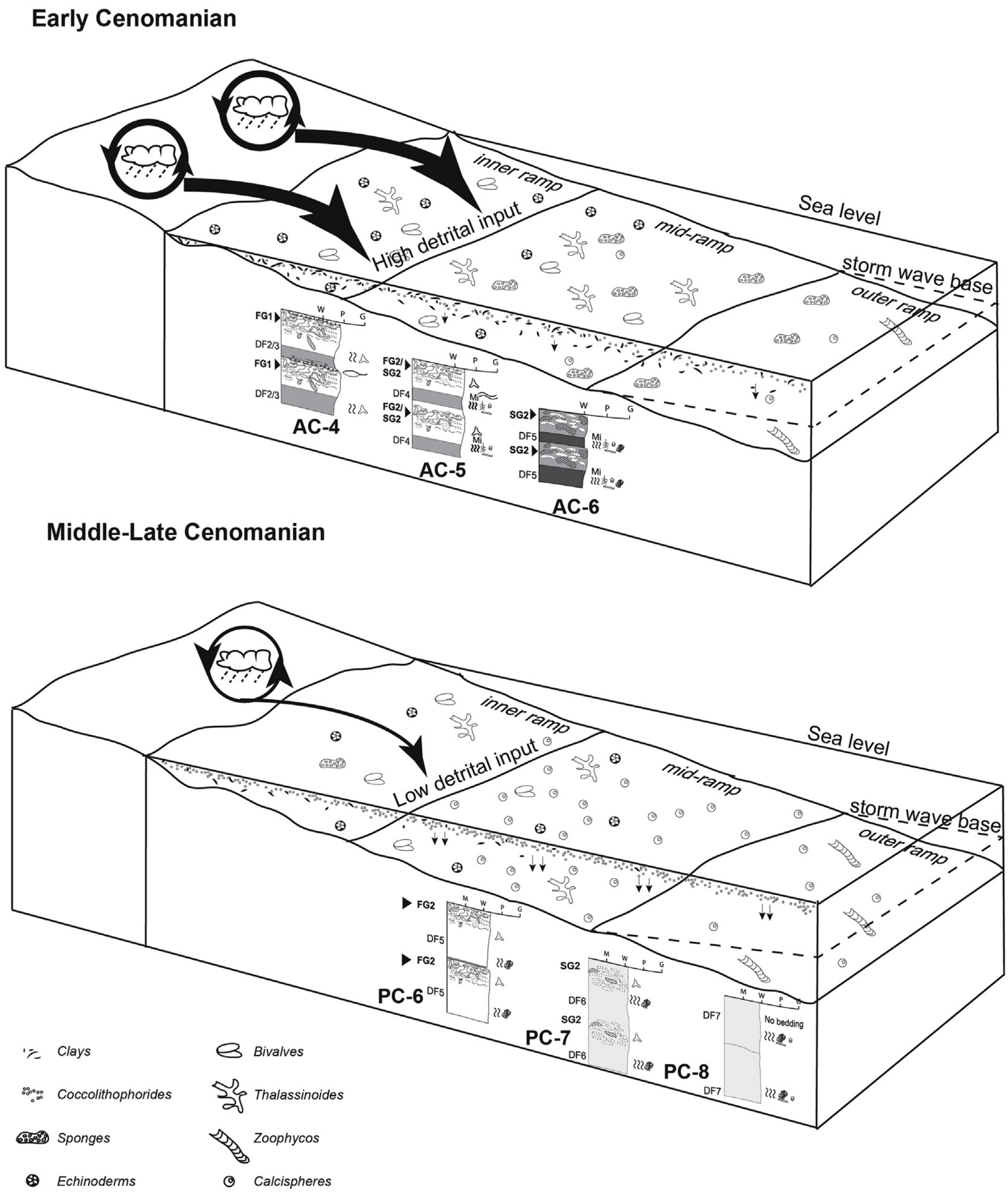

Fig. 5. Depositional environment reconstruction during early Cenomanian and middle/late Cenomanian.

porosity is reduced to 17–25%. Clay-rich microtextures, with a low degree of cementation (MT3 and 4) commonly displays very low permeability (below 0.2 mD) and high non-carbonate contents (16–37%).

Cap Blanc-Nez chalks cover a wide spectrum of uniaxial compressive strength (UCS) values, ranging from 7 to 32 MPa. They classify as extremely soft (< 9 MPa) to very hard (25–45 MPa) according to the classification of Mortimore and Fielding (1990). Porosity is known to be a controlling parameter on UCS in sedimentary rocks (e.g. Chang et al., 2006; Vernik et al., 1993). Regarding chalk samples from Cap Blanc-Nez, the best-fit correlation between porosity and UCS is exponential (Faÿ-Gomord et al., 2016b), and the coefficient of determination $R^2 = 0.63$ (Fig. 9). Dispersion of the data is a function of microtexture variation. Several authors have demonstrated that parameters such as cementation, grain contact and clay content control the geomechanical properties (e.g. Faÿ-Gomord et al., 2016b; Mortimore and Fielding, 1990; Schroeder, 2002). Some MT1 samples (Fig. 9) display very low strength ranging from 7 to 9 MPa, while cemented samples from MT2 and MT5 display values ranging from 11 to 32 MPa depending on the degree of cementation. Therefore, strength increases with increased cementation in this succession.

4.4. Mechanical stratigraphy

Fracture intensity strongly varies throughout the 70 m thick succession. The normalised average fracture spacing of each mechanical unit ranges from 18 to 232 cm, with coefficients of variation (Cv) ranging from 0.32 to 0.85 (Appendix 2). The low Cv (< 1) reflects the absence of clustering along the measured scanlines and quantifies the regularity of the fractures. Along the section, five zones (Z1 to Z5) with distinct mechanical behaviour can be differentiated (Fig. 10):

- Z1: The base of the lower Cenomanian, from 0 to 12 m on the lithology log, is characterised by successive half-metre to metre scale mechanical units (MU) from MU 1 to 9 (Fig. 10). Mechanical unit thickness ranges from 63 to 220 cm and fracture spacing ranges from 19 to 94 cm. Most sedimentary cycles (AC-cycles) represent

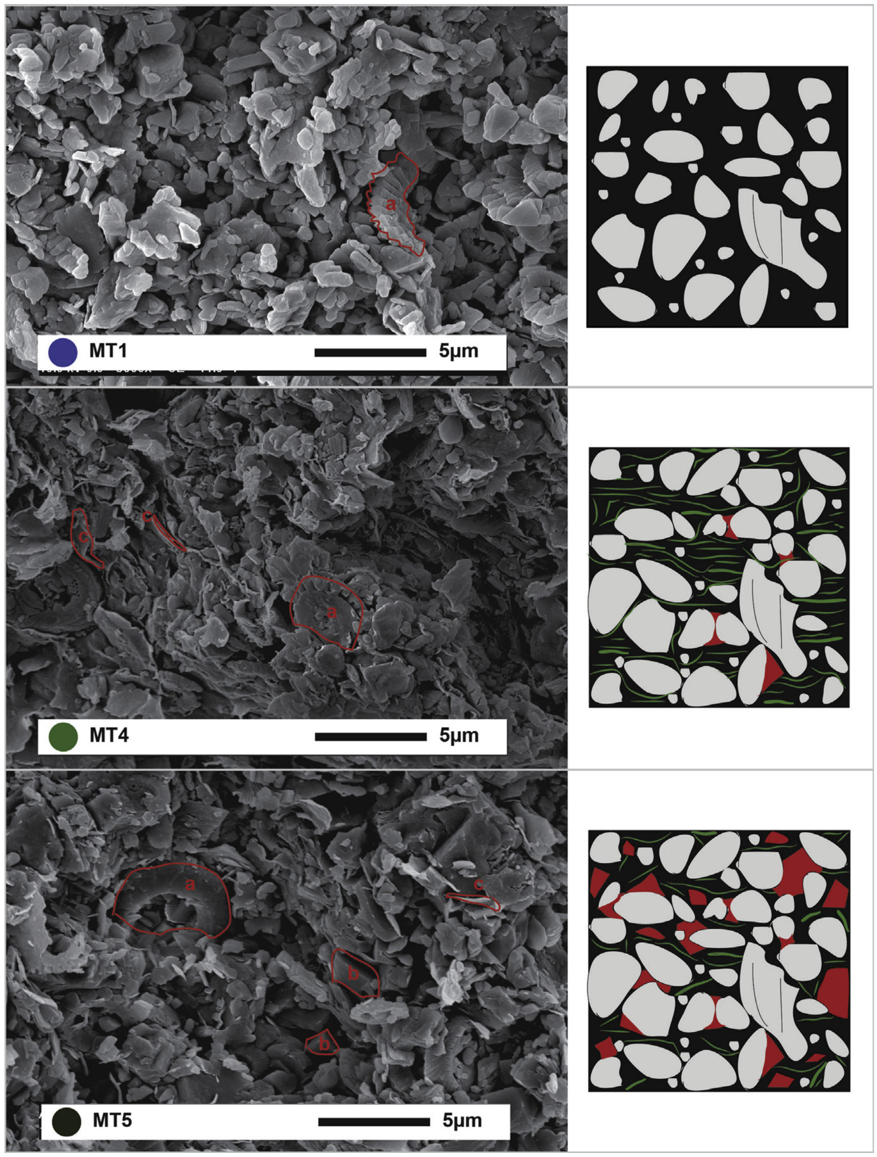

Fig. 6. SEM-microphotograph and schematic representation of three characteristic microtexture type (MT1) Pure chalk with visible interparticle porosity (MT4) Highly argillaceous chalk with clay flakes orientated parallel to the stratigraphy (MT5) Cemented argillaceous chalk displaying both clay flakes dispersed in the matrix and calcite cements. In green are the clay flakes and in red the cement crystals. (For interpretation of the references to colour in this figure legend, the reader is referred to the Web version of this article.)

single mechanical units. Between 20 and 58% of the fractures initiate between the firmground at the top of a cycle and the marly deposits at the base of the overlying one. Mechanical interfaces (MI) within this succession are mostly made of hardened bioturbated firmgrounds, in some cases made up of a layer of sponges affected by early cementation (MI 5/6, MI 7/8). On the mechanical interface MI 7/8 for instance 44% of fractures initiate or terminate, whereas 56% cross-cut the interface. In the field, a fracture trajectory either stops against a cemented sponge fossil or cross the mechanical interface avoiding sponges, highlighting the impact fossils may have on the strength of a mechanical interface.

- Z2: The first densely fractured zone (DFZ1) is observed from 12 to 26 m (Fig. 10) in the lower Cenomanian. The DFZ are characterised by large sigmoidal fractures which are confined to this stratigraphic interval. The fractures cross the entire DFZ at high angles and are deflected to lower angles towards the bottom and the top of the DFZ. The sigmoidal fractures are connected by a very dense fracture network (Fig. 11). The interface at the base of the DFZ corresponds to a clay layer and is characterised by a high amount of initiating fractures (e.g. 41% for DFZ1) at the interface.
- Z3: Middle Cenomanian, from 26 to 33 m, is characterised by the presence of two individual metre-thick firmgrounds of MT5 which behave as separate mechanical units (i.e. MU10 and MU12). Measurements show that 64% (MI DFZ1–10) and 31% (MI 11–12) of fractures are initiating at the basal interface, while 62% (MI 10–11) and 55% (MI 12–13) of the fractures terminate at the upper interface. This means that a major part of the fractures within firmgrounds are stratabound. They are thus poorly connected to the overall fracture network. The percentage of fractures terminating at the lower interface of a firmground is rather low (11 and 6% respectively), probably due to the fact that a firmground is sedimentologically marked by a gradual transition from regular chalk towards a more hardened chalk, characteristic of condensed surfaces associated with early sediment lithification. This explains the presence of stronger mechanical interfaces at the top of hiatal surfaces. Cv for MU10 and MU12 equals 0.54 and 0.65 respectively, illustrating rather regular and homogeneous fracture spacing.
- Z4: From 33 to 53 m, the insoluble residue is significantly lower and

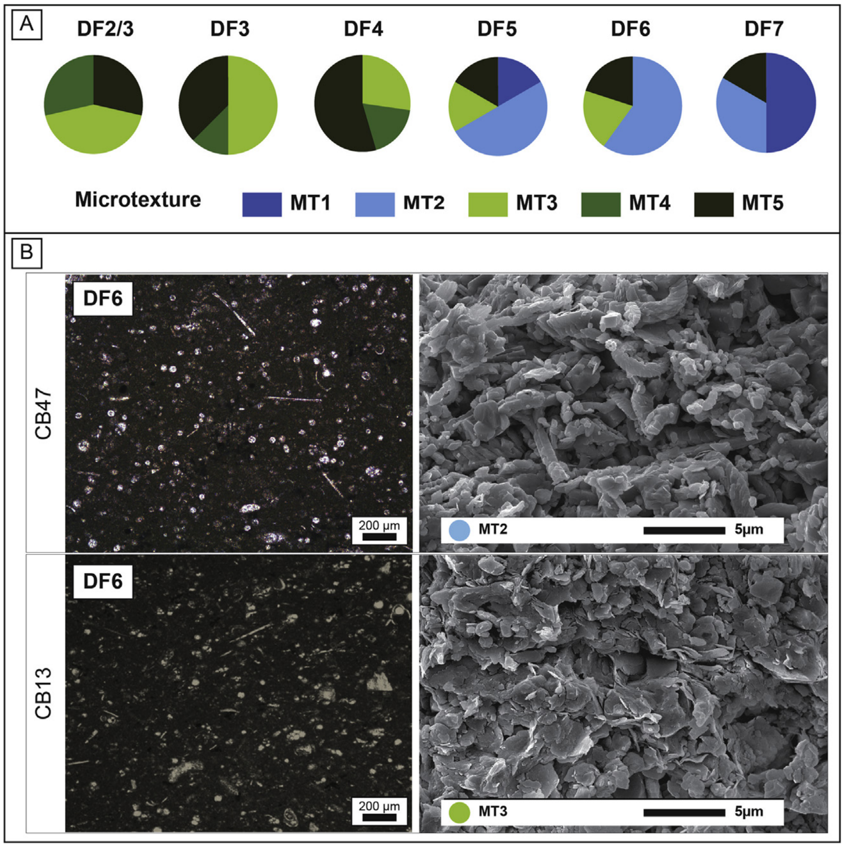

Fig. 7. (A) Pie charts of microtexture types plotted by depositional facies (B) Example of two samples that display similar depositional facies but different microtextures, CB47 and CB13. Relative to CB47, CB13 has been modified by pressure-dissolution that concentrated clays.

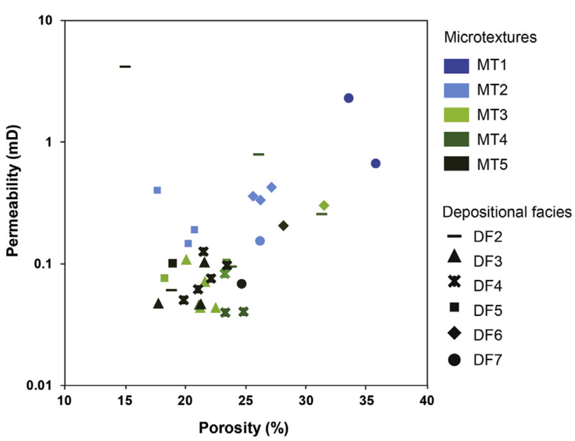

Fig. 8. Porosity versus permeability cross plot illustrating microtexture (colour) and depositional facies (shape) influences. (For interpretation of the references to colour in this figure legend, the reader is referred to the Web version of this article.)

chalk deposits are essentially characterised by an alternation of pure chalk and marl-seams, with poorly pronounced softgrounds or absence of hiatal surfaces (Fig. 3 E–F). However, in terms of mechanical stratigraphy those 30–50 cm thick pure chalk (PC-7) sedimentary cycles do not behave as separate entities. The thickness of the mechanical units range from 2 to 5.5 m, while fracture spacing varies from 117 to 232 cm, revealing very low fracture intensity compared to the rest of the Cenomanian succession. Mechanical interfaces bounding MU15 and MU16 are clay layers, described by Amédro and Robaszynski (2001) as stratigraphic marker-beds. However, MU17 unit corresponds to a distinct sedimentological unit semi-nodular chalk interval. Here the mechanical interfaces are defined by a strong contrast between the semi-nodular chalk defined by MT5 with an insoluble residue content of 12% and the surrounding chalk defined by MT2 with 6–7% of insoluble residue.

- Z5: A second densely fractured zone (DFZ2) is observed from 53 to 74 m in the upper Cenomanian. Like DFZ1, DFZ2 is characterised by large stratigraphically-confined sigmoidal fractures, connected by a very dense fracture network. The interface at the base of DFZ2 consists of a clay-rich layer, characterised by 60% of initiating fractures, mostly large stratabound sigmoidal fractures. This zone is mainly composed of pure chalk (PC-8) cycles where no hiatal surfaces nor bedding are observed.

The relationship between the mechanical unit thickness and the fracture spacing show a linear correlation with a coefficient of determination $R^2 = 0.91$ (Fig. 12) when the two major densely fractured zones are not taken into account. However, very few data are available for mechanical units thicker than 3 m (MU15, 16 and 17). For thinner mechanical units fracture saturation occurs, resulting in fracture spacing not decreasing below 18 cm (MU10). Therefore, a power or exponential correlation law would also fit the data, but the data set (only 18 mechanical units) is too limited to define preferential correlations. Instead, the focus of the study is given to the densely fractured zones, which behave as preferential fluid flow pathways and aquifer reservoirs. This is shown by the fresh water outlets visible on the outcrop (Fig. 11). If similar fracture zones would occur in hydrocarbon reservoirs, they would be potential preferential reservoir targets.

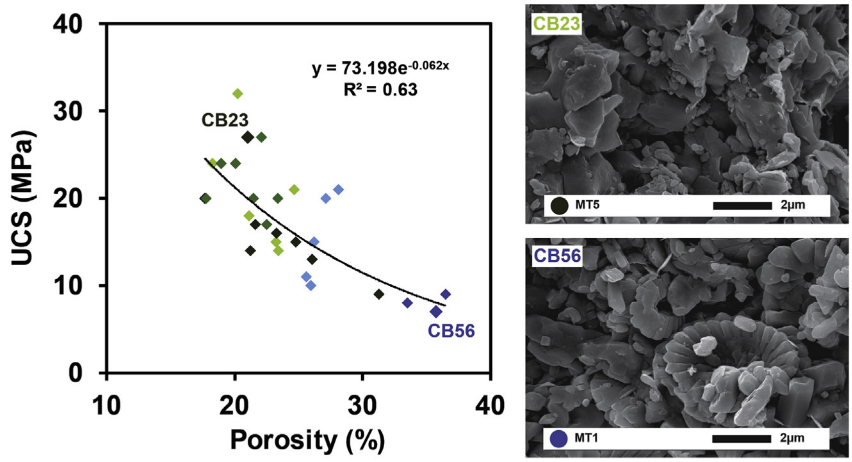

Fig. 9. Porosity versus uniaxial compressive strength (UCS) cross plot. SEM-microphotographs illustrate differences between a high-strength sample (CB23) with low interparticle porosity and calcite cements and a low-strength sample (CB56) with high interparticle porosity and punctic contact between grains.

5. Discussion

5.1. Microtextures: sedimentology and diagenesis

The diversity of chalk microtextures observed at Cap Blanc-Nez is shown Fig. 13. The two main factors controlling microtexture properties are depositional setting and subsequently diagenesis. The initial non-carbonate content is a key parameter, which controls burial diagenesis. Within pure chalk (MT1) a stabilized framework develops early during diagenesis and even more so in chalk affected by eogenetic processes such as hardground formation (MT2), resulting in limited grain to grain pressure dissolution during subsequent burial diagenesis. SEM-observations show that the degree of cementation of the matrix microtexture is higher in argillaceous chalk, especially chalk with an insoluble residue ranging from about 10 to 25%. The pressure dissolution processes are concentrated at grain to grain contacts, leading to cementation of the whole microtexture. Isolated rhombic calcite crystals and overgrowth cements are common, resulting in MT3 or MT5, where porosity loss results from both mechanical and chemical compaction (Fig. 13). However, samples with insoluble residue higher than 25% are less cemented and clay flakes are commonly orientated parallel to bedding, reflecting intense mechanical compaction. Mallon and Swarbrick (2008) noted that the effect of compaction can clearly be seen in the highly argillaceous chalk. They describe mechanical flattening, sometimes around more rigid features such as larger bioclasts. Such features are observed in MT4 samples and suggest a possible clay-content threshold value around 25% above which mechanical compaction dominates the loss in porosity.

In upper Cenomanian chalk of Cap Blanc-Nez, marl-seams are developed in slightly clay-rich chalks that contain about 5–10% insoluble residue. Marl-seams commonly overlie hiatal surfaces, characterised by a bioturbated layer in UK chalks (Kennedy and Garrison, 1975). Their origin, sedimentary versus diagenetic, is still debated (Wray and Jeans, 2014). Microtextural and field observations suggest that marl-seams result from burial diagenetic pressure-dissolution processes, which propagate laterally ensuing local concentration of insoluble residues. According to the model proposed by Westphal et al. (2000) and Westphal (2006) with regard to marl-limestone alternations, limestone beds are early cemented and thus mechanically stabilized. Moreover, marl interlayers are compacted and calcium carbonate is dissolved during burial diagenesis (Fig. 13, MT4). The limestone beds receive calcium carbonate resulting in cementation, occluding primary porosity (Fig. 13, MT2). According to Neugebauer (1973), pressure solution is dependent on the contact pressure between two grains, which in geotechnical terms can be expressed as the effective stress (σ') (Terzaghi, 1936), defined as:

$$\sigma' = \sigma - u$$

where σ is the total stress and u the pore fluid pressure.

Therefore, the amount of pressure solution is largely dependent on the pore fluid pressure. Hill (1987) suggested that the presence of clays in chalk may reduce the permeability significantly and thus prevent drainage, producing the undrained conditions required for pressure dissolution. Marl-seams are initially depositional features which are enhanced during diagenesis due to carbonate dissolution.

5.2. A multilayered reservoir

This study supports the idea that chalk behaves as a multi-layered reservoir, especially when argillaceous chalk levels are present. The overall behaviour of individual beds is controlled by both sedimentary and diagenetic processes, which significantly affect the fracture distribution. Mechanical stratigraphy highlights that mechanical interfaces controlling fracture propagation always correspond to stratigraphic bedding heterogeneities. They are caused by different sedimentological and eogenetic processes, which commonly correspond to either clay-rich layers or hiatal surfaces, whose ichnological features are characteristic of a firm substratum. Duperret et al. (2002) first described chalk as an aquifer controlled horizontally by the marls and vertically by poorly developed pre-existing joint systems. Hydrogeologists (Brouyère, 2006; Odling et al., 2013; Van den Daele et al., 2007) consider chalk as a dual-porosity reservoir, with both matrix and fracture porosity. However, chalk reservoirs are still commonly modelled as homogeneous systems in an oversimplified way. A full understanding of fluid flow in argillaceous chalk reservoir systems requires an integrated approach in the analyses and modelling of such reservoirs. In order to predict a fracture network from core analyses, mechanical interfaces and their origins must be identified.

In this study, stratigraphic surfaces acting as mechanical interfaces always display strong microtextural heterogeneities. These interfaces commonly display strong contrast in insoluble residue or in degree of cementation, whereas porosity values may remain similar. Top surfaces of firmgrounds for instance, which are highly cemented, always behave as mechanical interfaces. Interestingly, the matrix petrophysical properties of firmgrounds/hardgrounds qualify them as permeability barriers. Nevertheless, since they are intensively fractured, they probably behave rather as very permeable conduits, enhancing fluid flow.

However, not all stratigraphic heterogeneities act as mechanical interfaces in other types of carbonates (Graham Wall, 2006; Underwood et al., 2003). Marl-seams do not behave as mechanical interfaces and do

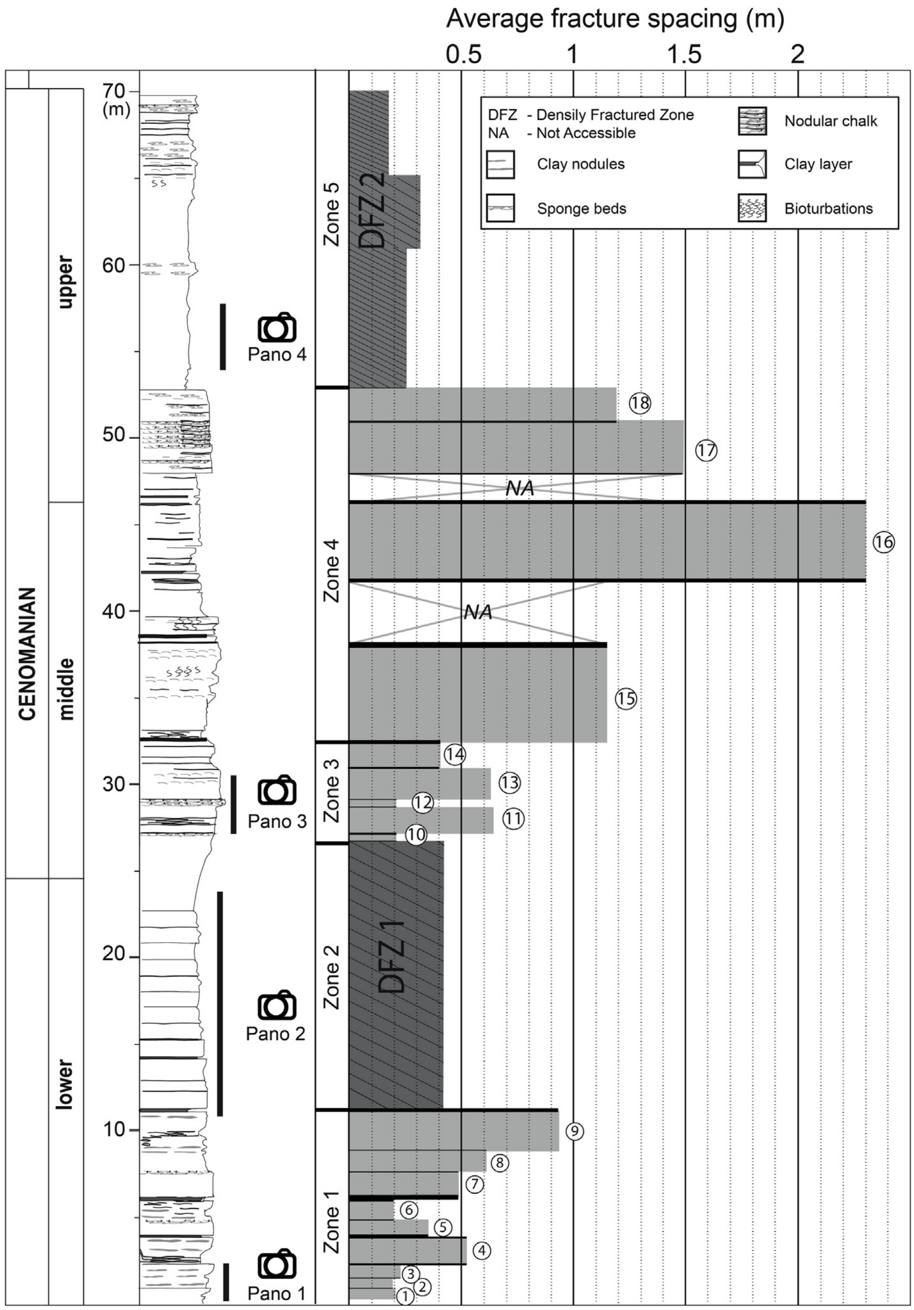

Fig. 10. Mechanical stratigraphy logging illustrating average fracture spacing for each mechanical unit. Location of the panoramas (Pano) detailed in Fig. 11 and scanlines data numbered from 0 to 18 are available in Appendix 2.

not confine bed-perpendicular fracture propagation. They form significant discontinuities within the succession, in terms of insoluble residue content. Graham-Wall (2006) reported similar observations within Cretaceous carbonate aquifers, where pressure-solution features acted as frictional interfaces. The solution seams allow fractures to propagate through them until they are sheared. They may terminate on bed-perpendicular fractures (Renshaw and Pollard, 1995; Cooke and Underwood, 2001). For a predictive approach, gamma ray spectra of boreholes could be used to define strong mechanical interfaces associated with clear contrasts between pure and argillaceous chalk.

5.3. Densely fractured zone: the role of clay content

The homogeneity of the pure chalk played a significant role in its fracturing behaviour (Rankin and May, 1996; Faÿ-Gomord et al., 2016b). Pure chalk sedimentary cycles do not display any strong heterogeneity which would have stopped fracture development. Thus, the pure chalk intervals correspond to Densely Fractured Zones (DFZ) acting as single mechanical units of dozens of metres thick, with large sigmoidal fractures confined to these units. Shear microstructures are observed in clay-rich layers bounding the DFZ. They indicate the occurrence of shear parallel bedding with a strong link with argillaceous content. The origin of the shear, however, is still being debated.

Clay flakes strongly influence the behaviour of the chalk submitted to sediment load and overburden pressure. Therefore, in a succession holding both argillaceous chalk and pure chalk intervals, different behaviours take place during compaction. During the first stage of burial diagenesis, clay-rich chalk probably underwent strong mechanical compaction, with a reorganization of the microtexture, while in pure chalk grain to grain contacts develop which finally stabilized the

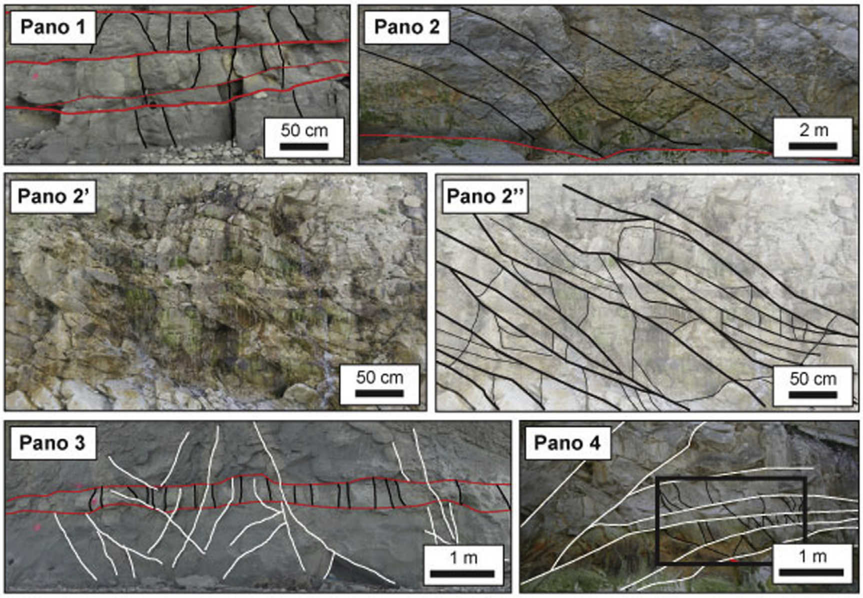

Fig. 11. Fracture networks of panoramas located on the log Fig. 10. In red, mechanical interfaces. Pano 1: Lower Cenomanian mechanical units constrained by sedimentary cycles, with mainly stratabound fractures. Pano 2: Densely fractured zone DFZ 1 with sigmoidal-shaped fractures. Note water resurgences on the zoom-in (Pano 2′), which reflect the preferential fluid flow in the DFZ. Pano 3: Many stratabound fractured confined to a 40 cm thick mechanical unit (MU12) defined by a firmground. Pano 4: Fracture network from DFZ2 with sigmoidal-shaped fractures (white) connected by a dense fracture network (black). (For interpretation of the references to colour in this figure legend, the reader is referred to the Web version of this article.)

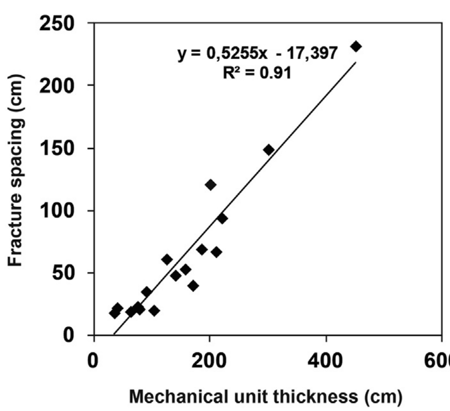

Fig. 12. Mechanical unit thickness versus fracture spacing cross plot.

framework. However, as the system reaches a critical stress-load, pure chalk fractured while clay-rich chalk was able to accommodate the stress, to a certain extent. Such a differential compaction origin for interstratal sliding has been first described by Wanless (1979) and is invoked by Hill (1987) to explain the 10 cm sigmoidal shaped fractures confined in the pure chalk beds of the Isle of Wight. These authors correlated fracture geometries to a stress field with a maximum principal stress angled normal to the bedding and with a shear component parallel to the bedding. Interstratal sliding, and local but multi-directional compaction stresses first described by Wanless (1979), are also dependent on the clay content. The DFZ are characterised by relatively pure and homogeneous chalk compared to the surrounding layered argillaceous chalk. Subhorizontal shear structures are observed in clay-rich layers, essentially above and below the DFZ. Our study shows contrasting UCS values ranging from 7 to 9 MPa within pure chalk, and from 20 to 32 MPa in argillaceous chalk. In addition, clay-rich chalks were proven to display a rather plastic behaviour, while pure chalks are more brittle (Rankin and May, 1996; Faÿ-Gomord et al., 2016b). The plastic behaviour of clays likely allowed them to accommodate part of the stress within argillaceous intervals, while the stress translated into intense fracturing within pure chalk.

However, the overall organization of the sigmoidal fractures pattern in the DFZ is not fully coherent with the hypothesis of a differential compaction origin. With a differential compaction on a regional scale, one would expect to observe a random distribution of the fractures due to horizontal isotropic stresses. Field measurements reveal that fractures in the DFZ are strikingly periodic with a constant azimuth and dip (~N120°, 50°). The overwhelming majority of fractures are northeast-dipping to the north of Escalles valley and southwest-dipping to the south of Escalles valley, with azimuths roughly parallel to the Cap Blanc Nez flexure axes (Fig. 1). These antithetic simple shears from either side of the flexure argue for a tectonic origin of the interstratal shear in the stratigraphic pile active during Paleogene inversion. Indeed, flexural slip is the dominant mechanism for accommodating folding in sequences of layered sedimentary rocks that display large competence contrasts (e.g., Ramsay, 1967; Chapple and Spang, 1974; Behzadi and Dubey, 1980; Tanner, 1989). Slip is typically concentrated on the limbs of the fold along horizons of low cohesion. Variations in cohesion along mechanical interfaces lead to nonuniform-slip distribution. The difference between slip vectors at the top and bottom of the pure chalk intervals is accommodated by the formation of recurrent opened sigmoidal fractures (parallel to flexure axes) that may then be preferential target zones in reservoirs, but may also behave as effective lateral flow pathways, where permeability is enhanced by intense fracturing.

Outcrop analogue observations are therefore crucial to understand the behaviour of subsurface pure/argillaceous chalk alternation. Pure chalk intervals may then be preferential target zones in reservoirs, but may also behave as lateral flow pathway, where permeability is enhanced by intense fracturing.

6. Conclusions

The multidisciplinary approach followed in this study provides a profound understanding of the properties of argillaceous and pure chalks and their fracturing behaviour. The integrated study unravels the close interrelationship between depositional setting and diagenesis, and how they both impact petrophysical, geomechanical and fracturing properties in argillaceous and pure chalk. It offers promising prospects for predicting chalk properties in the subsurface:

(1) Sedimentological, petrographic and petrophysical analyses indicate how the combination of the detrital input and grain-sorting together with pressure solution and cementation control the microtexture. Differences in microtextures related to deposition, are accentuated by diagenesis and thus constrain the petrophysical and geomechanical properties of the chalks.
(2) Insoluble residue plays a key role in the diagenetic imprint. Pure

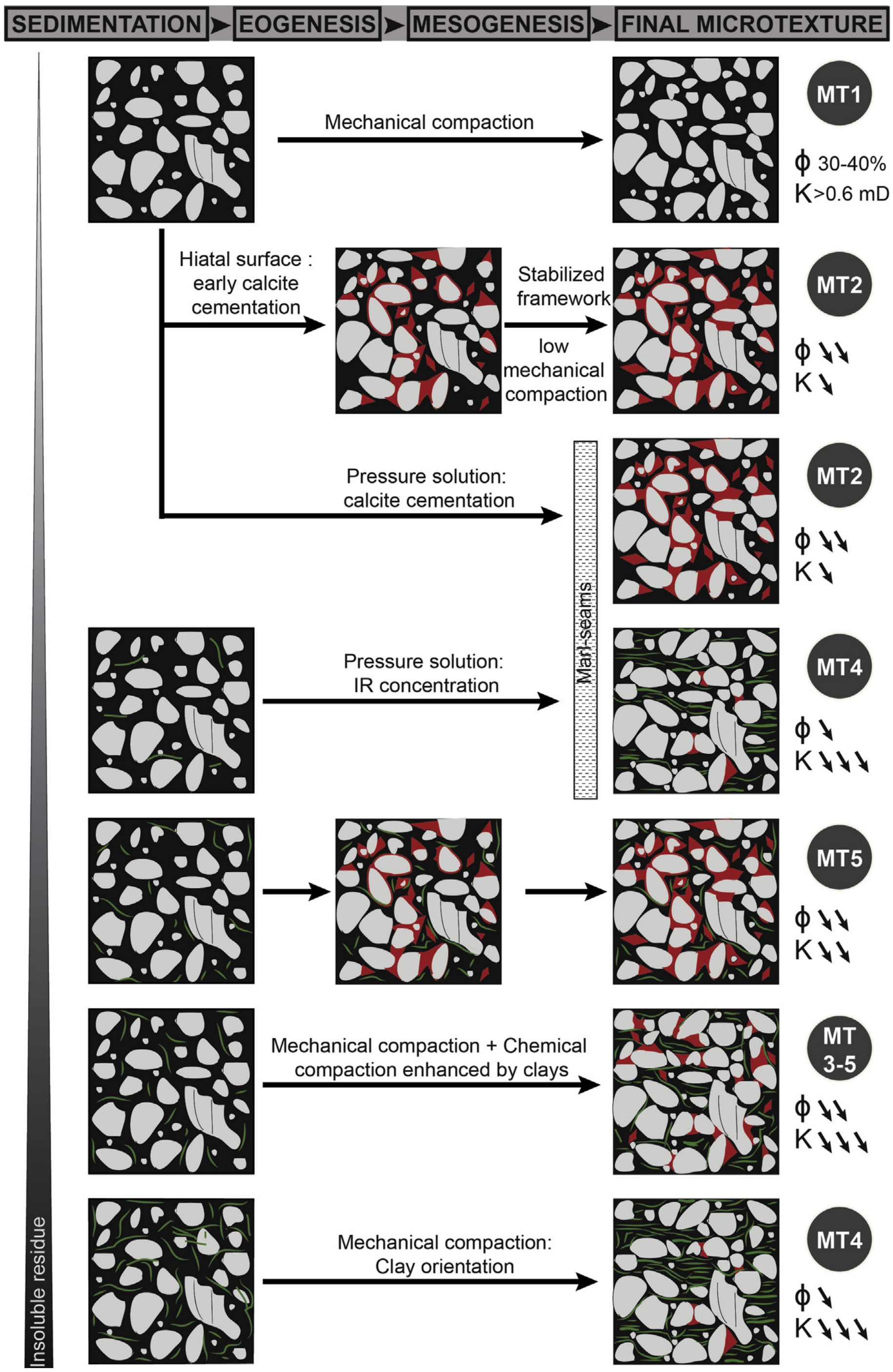

Fig. 13. Model for the influence of detrital input and diagenesis on chalk final microtexture.

chalk is only slightly affected by mechanical compaction developing a rigid framework with strong grain to grain contacts. Burial diagenesis resulted in the formation of pressure dissolution marl-seams, which develop in chalk intervals slightly enriched in clays. In chalk that contains 10 to about 25% of insoluble residue, clay flakes between grains enhance cementation within the interparticle porosity. However, from a certain threshold value of non-carbonate content above around 25% IR, chalks are poorly to non-cemented and mechanical compaction controls the microtexture, resulting in clay flakes being oriented parallel to the bedding.

(3) The assessment of the mechanical stratigraphy shows that mechanical interfaces are associated with lithological heterogeneities, yielding strong microtextural contrasts related to the non-carbonate content or/and degree of cementation. The mechanical units are thus defined either by deposition (sedimentary clay-rich layers, Milankovitch sedimentary-cyclicity) or diagenesis in the form of firmgrounds.

(4) The fracturing behaviour of about 10 m homogeneous pure chalk units differs significantly from the rest of the exposed succession. Large sigmoidal-shaped fractures are confined to those intervals, and a dense fracture network developed. Sliding with an apparent shear-stress component is observed at the mechanical interfaces. While plastic clay layers are able to accommodate part of the stress, homogeneous pure chalk displays a more brittle behaviour. The differential response resulted in densely fractured pure chalk intervals which may act as preferential fluid flow pathways in

subsurface settings due to their increased fracture permeability.

Acknowledgments

This study has been funded by TOTAL S.A., as part of a "Fractured Tight Chalk" project, including the PhD of Ophélie Faÿ-Gomord. Our thanks go to Yves Leroy (project leader, TOTAL S.A.) for the support he granted us throughout this study. We are thankful to DREAL Nord Pas de Calais for their sampling authorisations in the protected site of Cap Blanc-Nez. We like also to thank Herman Nijs (KU Leuven), for the preparation of the thin-sections, Elvira Vassilieva (KU Leuven) for her help during insoluble residue measurements, and Becki Scott (KU Leuven) for the critical reading of the manuscript. We are also very grateful to Francis Amédro (University of Burgundy) for his help and expertise during fieldwork in Cap Blanc-Nez (France). We are thankful for the valuable comments from the reviewers which significantly improved the quality of the manuscript.

Appendix A. Supplementary data

Supplementary data related to this article can be found at http://dx.doi.org/10.1016/j.marpetgeo.2018.03.037.

References

Agarwal, B., Hermansen, H., Sylte, J.E., Thomas, L.K., 2000. Reservoir characterization of Ekofisk field: a giant, fractured chalk reservoir in the Norwegian North Sea—history match. SPE Reservoir Eval. Eng. 3. http://dx.doi.org/10.2118/68096-PA.

Amédro, F., Robaszynski, F., 2001. Les craies cénomaniennes du Cap Blanc-Nez (France) au regard de la stratigraphie évènementielle. Extension géographique de niveaux repères du bassin anglo-parisien (Boulonnais, Kent, Normandie) à l'Allemagne du Nord. Bull. Trimest. Soc. Géol. Normandie Amis Mus. Havre 87, 9–29.

Amédro, F., Robaszynski, F., 1993. La Zone à Actinocamax plenus dans le Domaine boréal. Eléments de comparaison de la limite Cénomanien-Turonien entre les Domaines boréal et téthysien. Cretac. Res. 14, 487–494. https://doi.org/10.1006/cres.1993.1034.

Bailey, H., Gallagher, L., Hampton, M., Krabbe, M., Jones, B., Jutson, D., Moe, A., Nielsen, E.B., Petersen, N.W., Riis, F., Sawyer, D., Sellwood, B.W., Strand, T., Overli, P., Oxnevad, I., 1999. Joint Chalk Research Phase V: a Joint Chalk Stratigraphic Framework. Norwegian Petroleum Directorate (NPD), Stavanger.

Bear, J., 1993. Modeling flow and contaminant transport in fractured rocks. In: Flow and Contaminant Transport in Fractured Rock. Academic Press, Oxford, pp. 1–37. https://doi.org/10.1016/B978-0-12-083980-3.50005-X.

Behzadi, H., Dubey, A.K., 1980. Variation of interlayer slip in space and time during flexural slip folding. J. Struct. Geol. 2, 453–457.

Bergerat, F., Vandycke, S., 1994. Palaeostress analysis and geodynamical implications of Cretaceous-Tertiary faulting in Kent and the Boulonnais. J. Geol. Soc. Lond. 151, 439–448. http://dx.doi.org/10.1144/gsjgs.151.3.0439.

Bevan, T.G., Hancock, P.L., 1986. A late Cenozoic regional mesofracture system in southern England and northern France. J. Geol. Soc. Lond. 143, 355–362.

Briais, J., Guillocheau, F., Lasseur, E., Robin, C., Châteauneuf, J.J., Serrano, O., 2016. Response of a low-subsiding intracratonic basin to long wavelength deformations: the Palaeocene–early Eocene period in the Paris Basin. Solid Earth 7, 205–228. http://dx.doi.org/10.5194/se-7-205-2016.

Brouyère, S., 2006. Modelling the migration of contaminants through variably saturated dual-porosity, dual-permeability chalk. J. Contam. Hydrol. 82, 195–219. https://doi.org/10.1016/j.jconhyd.2005.10.004.

Brunet, M.-F., Le Pichon, X., 1982. Subsidence of the Paris Basin. J. Geophys. Res. Solid Earth 87, 8547–8560. http://dx.doi.org/10.1029/JB087iB10p08547.

Caine, J.S., Evans, J.P., Forster, C.B., 1996. Fault zone architecture and permeability structure. Geology 24, 1025–1028.

Chang, C., Zoback, M.D., Khaksar, A., 2006. Empirical relations between rock strength and physical properties in sedimentary rocks. J. Petrol. Sci. Eng. 51, 223–237.

Chapple, W.M., Spang, J.H., 1974. Significance of layer-parallel slip during folding of layered sedimentary rocks. Geol. Soc. Am. Bull. 85, 1523–1534.

Colbeaux, J.P., 1974. Mise en évidence d'une zone de cisaillement Nord-Artois. Acad. Sci. Paris 278, 1159–1161.

Cooke, M.L., Simo, J., Underwood, C., Rijken, P., 2006. Mechanical stratigraphic controls on fracture patterns within carbonates and implications for groundwater flow. Sediment. Geol. 184, 225–239. http://dx.doi.org/10.1016/j.sedgeo.2005.11.004.

Cooke, M.L., Underwood, C.A., 2001. Fracture termination and step-over at bedding interfaces due to frictional slip and interface opening. J. Struct. Geol. 23, 223–238. https://doi.org/10.1016/S0191-8141(00)00092-4.

Damholt, T., Surlyk, F., 2004. Laminated–bioturbated cycles in Maastrichtian chalk of the North Sea: oxygenation fluctuations within the Milankovitch frequency band. Sedimentology 51, 1323–1342. http://dx.doi.org/10.1111/j.1365-3091.2004.00672.x.

Deconinck, J.F., Amédro, F., Baudin, F., Godet, A., Pellenard, P., Robaszynski, F., Zimmerlin, I., 2005. Late Cretaceous palaeoenvironments expressed by the clay mineralogy of Cenomanian-Campanian chalks from the east of the Paris Basin. Cretac. Res. 26, 171–179. http://dx.doi.org/10.1016/j.cretres.2004.10.002.

Deconinck, J.F., Chamley, H., 1995. Diversity of smectite origins in Late Cretaceous sediments; example of chalks from northern France. Clay Miner. 30, 365 LP–379.

Deconinck, J.-F., Holtzappfel, T., Robaszynski, F., Amédro, F., 1989. Données minéralogiques, géochimiques et biologiques comparées dans les craies cénomaniennes à santoniennes du Boulonnais. Geobios 22, 179–188. https://doi.org/10.1016/S0016-6995(89)80055-5.

Doremus, C., 1978. Les craies du Nord de la France—corrélations entre la lithostratigraphie, la microstructure et les propriétés mécaniques. 3rd cycle doctorate thesis. Université de Lille I.

Downing, R.A., Price, M., Jones, G.P., 2005. The Hydrogeology of the Chalk of North-West Europe.

Duperret, A., Genterj, A., Mortimore, R.N., Delacourt, B., De Pomerai, M.R., 2002. Coastal rock cliff erosion by collapse at Puys, France: the role of impervious Marl seams within chalk of NW Europe. J. Coast Res. 18, 52–61.

Fabricius, I.L., 2007. Chalk: composition, diagenesis and physical properties. Geol. Soc. Den. Bull. 55, 97–128.

Fabricius, I.L., 2001. Compaction of microfossil and clay-rich sediments. Phys. Chem. Earth, A Solid Earth Geod. 26, 59–62. http://dx.doi.org/10.1016/S1464-1895(01)00023-0.

Fabricius, I.L., Røgen, B., Gommesen, L., 2007. How depositional texture and diagenesis control petrophysical and elastic properties of samples from five North Sea chalk fields. Petrol. Geosci. 13, 81–95. http://dx.doi.org/10.1144/1354-079306-707.

Faulkner, D.R., Jackson, C.A.L., Lunn, R.J., Schlische, R.W., Shipton, Z.K., Wibberley, C.A.J., Withjack, M.O., 2010. A review of recent developments concerning the structure, mechanics and fluid flow properties of fault zones. J. Struct. Geol. 32, 1557–1575. https://doi.org/10.1016/j.jsg.2010.06.009.

Faÿ-Gomord, O., Descamps, F., Tshibangu, J.-P., Vandycke, S., Swennen, R., 2016a. Unraveling chalk microtextural properties from indentation tests. Eng. Geol. 209, 30–43. http://dx.doi.org/10.1016/j.enggeo.2016.05.005.

Faÿ-Gomord, O., Soete, J., Katika, K., Galaup, S., Caline, B., Descamps, F., Lasseur, E., Lykke, I., Saïag, J., Swennen, R., Vandycke, S., 2016b. New insight into the microtexture of chalks from NMR analysis. Mar. Petrol. Geol. 75, 252–271. http://dx.doi.org/10.1016/j.marpetgeo.2016.04.019.

Garrison, R.E., 1981. Diagenesis of oceanic carbonate sediments. In: The Deep Sea Drilling Project. SEPM Society for Sedimentary Geology, pp. 181–207. http://dx.doi.org/10.2110/pec.81.32.0181.

Gennaro, M., Wonham, J.P., Sælen, G., Walgenwitz, F., Caline, B., Faÿ-Gomord, O., 2013. Characterization of dense zones within the danian chalks of the Ekofisk field, Norwegian North Sea. Petrol. Geosci. 19, 39–64.

Gillespie, P.A., Johnston, J.D., Loriga, M.A., McCaffrey, K.J.W., Walsh, J.J., Watterson, J., 1999. Influence of layering on vein systematics in line samples. Geol. Soc. Lond. Spec. Publ. 155, 35–56. http://dx.doi.org/10.1144/GSL.SP.1999.155.01.05.

Gillespie, P.A., Walsh, J.J., Watterson, J., Bonson, C.G., Manzocchi, T., 2001. Erratum to "Scaling relationships of joint and vein arrays from the Burren, Co. Clare, Ireland". J. Struct. Geol. 23, 1–2.

Gommesen, L., Fabricius, I.L., Mukerji, T., Mavko, G., Pedersen, J.M., 2007. Elastic behaviour of North Sea chalk: a well log study. Geophys. Prospect. 55, 307–322.

Gräfe, K.U., 1999. Foraminiferal evidence for Cenomanian sequence stratigraphy and palaeoceanography of the Boulonnais (Paris Basin, northern France). Palaeogeogr. Palaeoclimatol. Palaeoecol. 153, 41–70. http://dx.doi.org/10.1016/S0031-0182(99)00080-2.

Graham Wall, B.R., 2006. Influence of depositional setting and sedimentary fabric on mechanical layer evolution in carbonate aquifers. Sediment. Geol. 184, 203–224. https://doi.org/10.1016/j.sedgeo.2005.11.003.

Guillocheau, F., Robin, C., Allemand, P., Bourquin, S., Brault, N., Dromart, G., Friedenberg, R., Garcia, J.-P., Gaulier, J.-M., Gaumet, F., Grosdoy, B., Hanot, F., Le Strat, P., Mettraux, M., Nalpas, T., Prijac, C., Rigollet, C., Serrano, O., Grandjean, G., 2000. Meso-Cenozoic geodynamic evolution of the Paris Basin: 3D stratigraphic constraints. Geodin. Acta 13, 189–245. https://doi.org/10.1016/S0985-3111(00)00118-2.

Haq, B., Hardenbol, J., Vail, P., 1987. Chronology of fluctuating sea levels since the Triassic. Science 235, 1156–1167.

Hardman, R.F.P., 1982. Chalk reservoirs of the North Sea. Bull. Geol. Soc. Den. 30, 119–137.

Hill, H.P., 1987. Chalk solution structures in cores from deep sea drilling project leg 94. Initial Rep. Deep Sea Drill. Proj. 94 (1–2), 1129–1143. http://dx.doi.org/10.2973/dsdp.proc.94.143.1987.

Hjuler, M.L., Fabricius, I.L., 2009. Engineering properties of chalk related to diagenetic variations of Upper Cretaceous onshore and offshore chalk in the North Sea area. J. Petrol. Sci. Eng. 68, 151–170. http://dx.doi.org/10.1016/j.petrol.2009.06.005.

Homewood, P., Guillocheau, F., Eschard, R., Cross, T.A., 1992. Correlation haute résolution et stratigraphie génétique, une démarche intégrée. Bulletin des Centres de Recherches Exploration Production Elf Aquitaine, 16, 203Horsrud, P., 2001. Estimating mechanical properties of shale from empirical correlations. SPE Drill. Complet. 16, 68–73.

Jakobsen, F., Ineson, J.R., Kristensen, L., Stemmerik, L., 2004. Characterization and zonation of a marly chalk reservoir: the Lower Cretaceous Valdemar field of the Danish central Graben. Petrol. Geosci. 10, 21–33. http://dx.doi.org/10.1144/1354-079303-584.

Juignet, P., 1974. La transgression crétacée sur la bordure orientale du Massif armoricain-Aptien, Albien, Cénomanien de Normandie et du Maine. Le stratotype du Cénomanien. Thèse Univ. Caen.

Kennedy, W.J., 1987. Sedimentology of Late Cretaceous– Palaeocene chalk reservoirs,

North Sea central Graben. In: Brooks, J., Glennie, K.W. (Eds.), Petroleum Geology of North-West Europe. Graham and Trotman, London, pp. 469–481.
Kennedy, W.J., Garrison, R.E., 1975. Morphology and genesis of nodular chalks and hardgrounds in the Upper Cretaceous of southern England. Sedimentology 22, 311–386. http://dx.doi.org/10.1111/j.1365-3091.1975.tb01637.x.
Lasseur, E., Guillocheau, F., Robin, C., Hanot, F., Vaslet, D., Coueffe, R., Neraudeau, D., 2009. A relative water-depth model for the Normandy Chalk (Cenomanian-Middle Coniacian, Paris Basin, France) based on facies patterns of metre-scale cycles. Sediment. Geol. 213, 1–26. http://dx.doi.org/10.1016/j.sedgeo.2008.10.007.
Le Solleuz, A., Doin, M.-P., Robin, C., Guillocheau, F., 2004. From a mountain belt collapse to a sedimentary basin development: 2-D thermal model based on inversion of stratigraphic data in the Paris Basin. Tectonophysics 386, 1–27. https://doi.org/10.1016/j.tecto.2004.03.006.
Lindgreen, H., Fallick, E., Jakobsen, F., Springer, N., 2012. The tight Danian Ekofisk chalk reservoir formation in the south Arne field, North Sea: mineralogy and porosity properties. J. Petrol. Geol. 35, 291–309. http://dx.doi.org/10.1111/j.1747-5457.2012.00531.x.
Madsen, H.B., 2010. Silica diagenesis and its effect on porosity of upper Maastrichtian chalk - an example from the Eldfisk Field, the North Sea. Geol. Surv. Den. Greenl. Bull. 47–50.
Mallon, A.J., Swarbrick, R.E., 2002. A compaction trend for non-reservoir North Sea Chalk. Mar. Petrol. Geol. 19, 527–539. http://dx.doi.org/10.1016/S0264-8172(02)00027-2.
Mallon, A.J., Swarbrick, R.E., 2008. Diagenetic characteristics of low permeability, non-reservoir chalks from the Central North Sea. Mar. Petrol. Geol. 25, 1097–1108. http://dx.doi.org/10.1016/j.marpetgeo.2007.12.001.
Mansy, J.L., Manby, G.M., Averbuch, O., Everaerts, M., Bergerat, F., Van Vliet-Lanoe, B., Lamarche, J., Vandycke, S., 2003. Dynamics and inversion of the Mesozoic Basin of the Weald-Boulonnais area: role of basement reactivation. Tectonophysics 373, 161–179. http://dx.doi.org/10.1016/S0040-1951(03)00289-0.
Mortimore, R.N., Fielding, P.M., 1990. The relationship between texture, density and strength of chalk. Chalk 109–132.
Nelson, R.A., 1985. Geologic Analysis of Naturally Fractured Reservoirs, Contributions in Petroleum Geology & Engineering. Gulf Pub. Co., Book Division.
Neugebauer, J., 1973. The diagenetic problem of chalk. The role of pressure solution and pore fluid. Neues Jahrbuch Geol. Palaontol. Abhand. 143, 223–245.
Odling, N.E., West, L.J., Hartmann, S., Kilpatrick, A., 2013. Fractional flow in fractured chalk; a flow and tracer test revisited. J. Contam. Hydrol. 147, 96–111. https://doi.org/10.1016/j.jconhyd.2013.02.003.
Ramsay, J.G., 1967. Folding and Fracturing of Rocks. McGraw-Hill, New York, pp. 568.
Rankin, W.J., May, R.E., 1996. Geotechnical properties. In: Engineering Geology of the Channel Tunnel, Chapter 11. Thomas Telford Publishing, pp. 144–173. http://dx.doi.org/10.1680/egotct.20450.0011.
Renshaw, C.E., Pollard, D.D., 1995. An experimentally verified criterion for propagation across unbounded frictional interfaces in brittle, linear elastic materials. Int. J. Rock Mech. Min. Sci. Geomech. Abstr. 32, 237–249. https://doi.org/10.1016/0148-9062(94)00037-4.
Robaszynski, F., Amédro, F., 1986. The Cretaceous of the Boulonnais (France) and a comparison with the Cretaceous of Kent (United Kingdom). Proc. Geol. Assoc. 97, 171–208. http://dx.doi.org/10.1016/S0016-7878(86)80067-0.
Robaszynski, F., Gale, A., Juignet, P., Amédro, F., Hardenbol, J., 1998. Sequence stratigraphy in the Upper Cretaceous of the Anglo-Paris Basin: exemplified by the Cenomanian stage. Soc. Econ. Paleontol. Mineral. Soc. Sediment. Geol. Spec. Publ. 60, 363–386.
Røgen, B., Fabricius, I.L., 2002. Influence of clay and silica on permeability and capillary entry pressure of chalk reservoirs in the North Sea. Petrol. Geosci. 8, 287–293. http://dx.doi.org/10.1144/petgeo.8.3.287.
Rustichelli, A., Tondi, E., Agosta, F., Cilona, A., Giorgioni, M., 2012. Development and distribution of bed-parallel compaction bands and pressure solution seams in carbonates (Bolognano Formation, Majella Mountain, Italy). J. Struct. Geol. 37, 181–199. https://doi.org/10.1016/j.jsg.2012.01.007.
Scholle, P.A., 1977. Chalk diagenesis and its relation to petroleum exploration; oil from chalks, a modern miracle? Am. Assoc. Petrol. Geol. Bull. 61, 982–1009.
Scholle, P.A., Albrechtsen, T., Tirsgaard, H., 1998. Formation and diagenesis of bedding cycles in uppermost Cretaceous chalks of the Dan field, Danish North Sea. Sedimentology 45, 223–243. http://dx.doi.org/10.1046/j.1365-3091.1998.0148e.x.
Schroeder, C., 2002. Du coccolithe au réservoir pétrolier. PhD thesis. University of Liège.
Tanner, P.W.G., 1989. The flexural-slip mechanism. J. Struct. Geol. 11, 635–655.
Taylor, S.R., Lapre, J.F., 1987. North Sea chalk diagenesis: its effect on reservoir location and properties. In: Brooks, J., Glennie, K.W. (Eds.), Petroleum Geology of North-West Europe. Graham and Trotman, London, pp. 483–495.
Terzaghi, K., 1936. The shearing resistance of saturated soils and the angle between the planes of shear. First Int. Conf. Soil Mech. Found. Eng., Harvard Univ. 1, 54–56.
Travis, B.J., 1984. TRACR3D: a Model of Flow and Transport in Porous/fractured Media. Rep. LA-9667-MS. Los Alamos Natl. Lab, Los Alamoos, NM, United States.
Underwood, C.A., Cooke, M.L., Simo, J.A., Muldoon, M.A., 2003. Stratigraphic controls on vertical fracture patterns in Silurian dolomite, northeastern Wisconsin. Am. Assoc. Petrol. Geol. Bull. 87, 121–142.
Van den Daele, G.F.A., Barker, J.A., Connell, L.D., Atkinson, T.C., Darling, W.G., Cooper, J.D., 2007. Unsaturated flow and solute transport through the Chalk: tracer test and dual permeability modelling. J. Hydrol. 342, 157–172. https://doi.org/10.1016/j.jhydrol.2007.05.021.
Vandycke, S., 2002. Palaeostress records in Cretaceous formations in NW Europe: extensional and strike-slip events in relationships with Cretaceous-Tertiary inversion tectonics. Tectonophysics 357, 119–136. http://dx.doi.org/10.1016/S0040-1951(02)00365-7.
Vandycke, S., Bergerat, F., 1992. Tectonique de failles et paléocontraintes dans les formations crétacées du Boulonnais (N France). Bull. Soc. Géol. Fr. 163, 553–560.
Vejbæk, O.V., 2002. Reservoir characterization of the roar gas field, Danish North Sea. Petrol. Geosci. 8, 71–87. http://dx.doi.org/10.1144/petgeo.8.1.71.
Vermilye, J.M., Scholz, C.H., 1998. The process zone: a microstructural view of fault growth. J. Geophys. Res. Solid Earth 103, 12223–12237. http://dx.doi.org/10.1029/98JB00957.
Vernik, L., Bruno, M., Bovberg, C., 1993. Empirical relations between compressive strength and porosity of siliciclastic rocks. Int. J. Rock Mech. Min. Sci. Geomech. 30, 677–680. https://doi.org/10.1016/0148-9062(93)90004-W.
Wanless, H.R., 1979. Limestone response to stress; pressure solution and dolomitization. J. Sediment. Res. 49, 437 LP–462.
Wendler, J., Gräfe, K.U., Willems, H., 2002. Reconstruction of mid-Cenomanian orbitally forced palaeoenvironmental changes based on calcareous dinoflagellate cysts. Palaeogeogr. Palaeoclimatol. Palaeoecol. 179, 19–41. http://dx.doi.org/10.1016/S0031-0182(01)00366-2.
Westphal, H., 2006. Limestone-marl alternations as environmental archives and the role of early diagenesis: a critical review. Int. J. Earth Sci. 95, 947–961. http://dx.doi.org/10.1007/s00531-006-0084-8.
Westphal, H., Head, M.J., Munnecke, A., 2000. Differential diagenesis of rhythmic limestone alternations supported by palynological evidence. J. Sediment. Res. 70, 715–725. http://dx.doi.org/10.1306/2DC40932-0E47-11D7-8643000102C1865D.
Wray, D.S., Jeans, C.V., 2014. Chemostratigraphy and provenance of clays and other non-carbonate minerals in chalks of Campanian age (Upper Cretaceous) from Sussex, southern England. Clay Miner. 49, 327–340.